bioRxiv preprint doi: https://doi.org/10.1101/2021.04.09.439171; this version posted April 10, 2021. The copyright holder for this preprint (which was not certified by peer review) is the author/funder, who has granted bioRxiv a license to display the preprint in perpetuity. It is made available under aCC-BY 4.0 International license.

Rad53 checkpoint kinase regulation of DNA replication fork rate via Mrc1 phosphorylation

Allison W. McClure[1] and John F.X. Diffley[1,*]

[1] Chromosome Replication Laboratory
The Francis Crick Institute, 1 Midland Road, London, NW1 1AT

*Corresponding Author
john.diffley@crick.ac.uk
Tel: +44 (0) 203 796 1833

Running title: (Optional)

bioRxiv preprint doi: https://doi.org/10.1101/2021.04.09.439171; this version posted April 10, 2021. The copyright holder for this preprint (which was not certified by peer review) is the author/funder, who has granted bioRxiv a license to display the preprint in perpetuity. It is made available under aCC-BY 4.0 International license.

Summary

The Rad53 DNA checkpoint protein kinase plays multiple roles in the budding yeast cell response to DNA replication stress. Key amongst these is its enigmatic role in safeguarding DNA replication forks. Using DNA replication reactions reconstituted with purified proteins, we show Rad53 phosphorylation of Sld3/7 or Dbf4-dependent kinase blocks replication initiation whilst phosphorylation of Mrc1 or Mcm10 slows elongation. Mrc1 phosphorylation is necessary and sufficient to slow replication forks in complete reactions; Mcm10 phosphorylation can also slow replication forks, but only in the absence of unphosphorylated Mrc1. Mrc1 stimulates the unwinding rate of the replicative helicase, CMG, and Rad53 phosphorylation of Mrc1 prevents this. We show that a phosphorylation-mimicking Mrc1 mutant cannot stimulate replication *in vitro* and partially rescues the sensitivity of a *rad53* null mutant to genotoxic stress *in vivo*. Our results show that Rad53 protects replication forks in part by antagonising Mrc1 stimulation of CMG unwinding.

Introduction

In response to DNA replication stress such as low nucleotide levels or DNA damage, a cascade of events is orchestrated by the DNA replication checkpoint to ensure genome protection. DNA replication stress is detected by proteins that activate the apical protein kinase Mec1 in *Saccharomyces cerevisiae* (ATR in humans) (Pardo et al., 2017; Saldivar et al., 2017). Mec1 then activates the effector protein kinase Rad53 through two mediator proteins, Rad9 and Mrc1. Active Rad53 coordinates a broad response to promote cell survival by regulating damage-dependent transcription, cell cycle, deoxyribonucleotide triphosphate (dNTP) levels, and replication origin firing (Bastos de Oliveira et al., 2012; Krishnan et al., 2004; Paulovich and Hartwell, 1995; Santocanale and Diffley, 1998; Travesa et al., 2012; Zegerman and Diffley, 2010; Zhao et al., 1998). In addition, Rad53 plays an essential role in stabilising stalled replication forks, allowing them to restart replication, and

bioRxiv preprint doi: https://doi.org/10.1101/2021.04.09.439171; this version posted April 10, 2021. The copyright holder for this preprint (which was not certified by peer review) is the author/funder, who has granted bioRxiv a license to display the preprint in perpetuity. It is made available under aCC-BY 4.0 International license.

promoting replication through damaged templates (Lopes et al., 2001; Tercero and Diffley, 2001; Tercero et al., 2003).

Wild-type cells progress very slowly through S phase in response to the DNA damaging agent MMS, but much faster in *rad53* or *mec1* mutant cells (Paulovich and Hartwell, 1995). The slow S phase progression in wild type cells is mainly due to checkpoint-dependent inhibition of origin firing (Tercero et al., 2003; Zegerman and Diffley, 2010). Rad53 inhibits origin firing through multiple, redundant phosphorylation events of two essential firing factors, Sld3 and Dbf4; non-phosphorylatable mutants of Sld3 and Dbf4, when combined, show the same fast progression through S phase as *rad53* mutants (Zegerman and Diffley, 2010). However, unlike *rad53* mutants, the non-phosphorylatable *sld3, dbf4* double mutant does not show enhanced sensitivity to replication stress consistent with the idea that regulation of fork stability, rather than origin firing by Rad53 is crucial for cell viability. The Rad53 targets involved in regulating replication fork stability are currently unclear, but several studies have implicated the Mec1-Rad53 checkpoint in replication fork slow-down in response to replication stress suggesting there may be a link between replication fork rate and stability (Bacal et al., 2018; Kumar and Huberman, 2009; Mutreja et al., 2018; Seiler et al., 2007).

Mrc1, and its human counterpart, Claspin, were initially characterised as mediators of the replication checkpoint. Mrc1 and a second mediator, Rad9, act redundantly in activating Rad53 after replication stress and the *mrc1*^{17AQ} mutant, which cannot be phosphorylated by Mec1, does not mediate Rad53 activation. In addition to its role in Rad53 activation, Mrc1 has a genetically separable role in regulating replisome progression in the absence of DNA damage. *mrc1*Δ cells progress slowly through S phase whilst *mrc1*^{17AQ} cells show normal S phase progression (Osborn and Elledge, 2003), and, conversely, cells with C-terminal truncations of Mrc1 that can still activate the checkpoint with near normal kinetics show slow S phase progression (Naylor et al., 2009). Mrc1, along with two associated proteins Csm3 and Tof1 (Tipin/Timeless in human cells), has also been shown to stimulate replication fork

bioRxiv preprint doi: https://doi.org/10.1101/2021.04.09.439171; this version posted April 10, 2021. The copyright holder for this preprint (which was not certified by peer review) is the author/funder, who has granted bioRxiv a license to display the preprint in perpetuity. It is made available under aCC-BY 4.0 International license.

rates *in vitro* (Lewis et al., 2017; Yeeles et al., 2017). Mrc1 associates with replication forks in S phase and has contacts with multiple replisome components (Bando et al., 2009; Baretić et al., 2020; Gambus et al., 2006; Katou et al., 2003; Komata et al., 2009; Lou et al., 2008), but how Mrc1 regulates fork progression is unclear. Here, we show that the ability of Mrc1 to stimulate replication is inhibited by Rad53 phosphorylation, implicating Mrc1 as both a mediator and a target of the checkpoint.

Results

Rad53 inhibition of origin firing in vitro via Dbf4 and Sld3

To understand in molecular detail how Rad53 regulates DNA replication, we have exploited the reconstitution of DNA replication with purified budding yeast proteins. In these experiments, the MCM double hexamers were assembled onto a 10.6 kb plasmid DNA template, then phosphorylated with Dbf4-dependent kinase (DDK), and finally firing factors, DNA polymerases, and accessory factors were added to initiate DNA replication. We followed replication progression by separating the products on alkaline agarose gels to visualise incorporation of radiolabeled dCTP. Rad53 inhibits late origin firing in vivo by phosphorylating two substrates: Dbf4 and Sld3 (Zegerman and Diffley, 2010). To determine if their phosphorylation directly inhibits their ability to promote replication, we pre-phosphorylated each individually with Rad53 and added them to replication reactions. To do this, we used Rad53 and the kinase-dead Rad53 mutant (K227A, D339A) purified after expression in *E.coli*. Rad53 expressed in *E.coli* is hyper-phosphorylated as previously shown (Gilbert et al., 2001), whilst the kinase dead mutant is not (Fig S1A). As shown in Figure 1A, pre-incubation of DDK with ATP caused a small shift in Dbf4 mobility in SDS-PAGE even in the absence of Rad53, presumably reflecting autophosphorylation (Francis et al., 2009; Kihara et al., 2000). However, there was a further shift of Dbf4 in the presence of wild type Rad53, which was not seen with the kinase dead Rad53. Figure 1B shows that DDK pre-phosphorylated with Rad53 was unable to promote replication (lane 3), while pre-incubation of DDK with ATP alone (lane 2) or with ATP and the kinase-dead Rad53 mutant

bioRxiv preprint doi: https://doi.org/10.1101/2021.04.09.439171; this version posted April 10, 2021. The copyright holder for this preprint (which was not certified by peer review) is the author/funder, who has granted bioRxiv a license to display the preprint in perpetuity. It is made available under aCC-BY 4.0 International license.

(lane 4) had no effect on replication. Whilst this work was in progress, Wahab and Remus showed that, in their system, binding of Rad53 to Dbf4 is sufficient to inhibit its ability to interact with the MCM double hexamer (Abd Wahab and Remus, 2020). In our hands, the kinase dead Rad53 did not inhibit replication. Moreover, preincubation of wild type Rad53 and DDK without ATP did not lead to inhibition. These results suggest that phosphorylation is required, which is consistent with previous genetic analysis showing that mutation of phosphorylation sites in Dbf4 prevented Rad53 inhibition (Zegerman and Diffley, 2010).

To test whether Rad53 also inhibited Sld3, we took a similar approach by pre-incubating Sld3/7 with Rad53 prior to addition to the replication reaction. Similar to DDK, pre-incubation of Sld3/7 with Rad53 and ATP resulted in reduced mobility of Sld3 in SDS-PAGE (Fig 1C) and inhibition of replication (Fig 1D, Fig S1B). This Rad53 inhibition of Sld3/7 was dependent on its kinase activity because the kinase defective mutant did not inhibit replication (lane 3, Fig 1D) and because pre-incubation without ATP did not inhibit replication (lane 5, Fig 1D). As a further control, if Sld3/7 and Rad53 were pre-incubated separately (lane 4, Fig 1D) replication was not inhibited. This also shows that Rad53 does not inhibit replication initiation when added together with the firing factors: presumably, replication initiates before Rad53 has time to phosphorylate and inhibit Sld3 and DDK. Taken together, these results show that phosphorylation of DDK or Sld3/7 can block initiation, consistent with previous results *in vivo* (Zegerman and Diffley, 2010).

Rad53 inhibition of replication elongation via Mrc1 and Mcm10

Next, we wanted to determine whether Rad53 affected replication elongation. We pre-incubated the elongation factor mix (RPA, Ctf4, TopoI, Csm3/Tof1, Mrc1, Polα, and Mcm10) with Rad53 and added this to reactions after MCM loading, DDK phosphorylation, and firing factor addition. We stopped the reactions at early time points so that any effects of elongation could be more easily seen by the size of the leading strand replication products. Figure 2A shows that the sizes of leading strand products were reduced after Rad53

bioRxiv preprint doi: https://doi.org/10.1101/2021.04.09.439171; this version posted April 10, 2021. The copyright holder for this preprint (which was not certified by peer review) is the author/funder, who has granted bioRxiv a license to display the preprint in perpetuity. It is made available under aCC-BY 4.0 International license.

phosphorylation. Figure 2B shows that these reductions correspond to a decrease in replication fork rate from about 0.7 kb/min to 0.4 kb/min.

Mrc1 and Csm3/Tof1 (M/C/T) are non-essential proteins known to directly stimulate replication fork rate (Yeeles et al., 2017). Their inactivation by Rad53, therefore, could provide an explanation for the reduction in fork rate caused by Rad53. Indeed, both Mrc1 and Csm3 (but not Tof1) exhibited reduced mobility in SDS-PAGE after incubation with Rad53 but not Rad53^{KD} (Fig 2C), indicating that Rad53 can phosphorylate these proteins. When M/C/T were pre-incubated with wild type Rad53, but not Rad53^{KD}, leading strand product size after 7 minutes of replication was decreased (Fig 2D). This leading strand product size was decreased when Mrc1 was incubated with Rad53 but not when Csm3/Tof1 was incubated with Rad53 (Fig 2D). These data indicate that phosphorylation of Mrc1 alone is sufficient to slow replication.

To determine whether phosphorylation of Mrc1 is necessary for Rad53 to slow replication, we pre-incubated all of the elongation factors, except Mrc1, with Rad53 prior to replication. Addition of Mrc1 separately completely rescued the reduction in replication speed by Rad53 (Fig 3A). Together with the previous experiments, we conclude that Rad53 phosphorylation of Mrc1 is necessary and sufficient to explain the slowing of replication rate by Rad53.

It has recently been shown that Rad53 can inhibit the already slow rate of replication fork progression in the absence of M/C/T (Devbhandari and Remus, 2020), which led these authors to conclude that Rad53 inhibition of fork rate does not require M/C/T. To investigate this apparent discrepancy further, we pre-incubated the mixture of elongation factors lacking M/C/T (RPA, Ctf4, TopoI, Polα, and Mcm10) with Rad53. Consistent with this previous work (Devbhandari and Remus, 2020), the presence of Rad53 reduced replication rate in the absence of M/C/T (Fig 3B, compare lanes 7-9 with 10-12). However, when unphosphorylated M/C/T was added to the reaction separately from the pre-incubated elongation protein mix, replication speed was completely rescued to the rate seen in the

bioRxiv preprint doi: https://doi.org/10.1101/2021.04.09.439171; this version posted April 10, 2021. The copyright holder for this preprint (which was not certified by peer review) is the author/funder, who has granted bioRxiv a license to display the preprint in perpetuity. It is made available under aCC-BY 4.0 International license.

absence of Rad53 (Fig 3B, lanes 13-15). From this we conclude that, in agreement with previous results, Rad53 can inhibit elongation via some target(s) other than M/C/T; however, this inhibition is only seen when unphosphorylated M/C/T is absent.

Mcm10 stimulates replication fork rate in the absence of Mrc1, but not in its presence (Langston et al., 2017; Lõoke et al., 2017), so inactivation of Mcm10 by Rad53 could explain our results. Incubation of Mcm10 with Rad53 reduced Mcm10 mobility in SDS-PAGE (Fig 3C) consistent with Rad53 phosphorylation of Mcm10. As shown in Figure 3D, incubation of Mcm10 with Rad53 reduced fork rate in the absence of Mrc1 (Fig 3D lanes 4 and 5) or in the presence of phosphorylated Mrc1 (Fig 3D lanes 2 and 3) but did not affect fork rate in the presence of unphosphorylated Mrc1 (Fig 3E). Interestingly, whilst pre-phosphorylation of Mcm10 with Rad53 affects its ability to accelerate fork rate, it did not inhibit replication initiation, suggesting that these functions of Mcm10 are separable.

Mrc1 regulation of replication rate

How Mrc1 supports fast replication speed is not well understood. Mrc1 has many contacts with Polε (Lou et al., 2008), and Mrc1 stimulates DNA replication when Polε is synthesising the leading strand (Fig 4A and (Yeeles et al., 2017)). Mrc1 could, therefore, directly stimulate DNA synthesis by Polε (Zhang et al., 2018). We tested this idea by using a truncation of the catalytic domain of Polε (Yeeles et al., 2017; Zhou et al., 2017), which supports CMG formation but does not synthesise DNA. In these reactions, Polα is the only DNA polymerase, and Mrc1 still stimulates replication rate (Fig 4B). In addition, Mrc1 can stimulate DNA replication when Polδ is synthesising the leading strand (Fig 4C and (Yeeles et al., 2017)). Further, Rad53 inhibits Mrc1 stimulation of replication rate in all three conditions (Fig 4A-C). Therefore, Mrc1 can stimulate DNA synthesis regardless of which DNA polymerase is synthesising the leading strand. Moreover, Rad53 prevents Mrc1 stimulation regardless of which polymerase is synthesising the leading strand.

We next asked if Mrc1 can directly stimulate the activity of the CMG helicase. Using the appearance of an underwound form of circular plasmid (form U*) as a measure of CMG

bioRxiv preprint doi: https://doi.org/10.1101/2021.04.09.439171; this version posted April 10, 2021. The copyright holder for this preprint (which was not certified by peer review) is the author/funder, who has granted bioRxiv a license to display the preprint in perpetuity. It is made available under aCC-BY 4.0 International license.

helicase activity, Devbhandari and Remus have recently shown that more U* product is generated in reactions containing M/C/T than in reactions lacking M/C/T (Devbhandari and Remus, 2020). This could indicate that M/C/T stimulates the rate of unwinding by CMG, or that M/C/T increases the ultimate extent of unwinding, or both. To distinguish these possibilities, we developed a new and quantitative assay to measure CMG activity (Fig 4D). Unwinding of double stranded DNA renders it resistant to cleavage by restriction endonucleases. The fraction of double- and single-stranded DNA can then be determined using qPCR with primers flanking restriction sites (Zierhut and Diffley, 2008). We constructed a linear DNA template with an origin of replication near one end and cassettes containing 4 tandem MseI restriction enzyme sites at 200 bp, 500 bp, 1000 bp, 1500 bp, and 2000 bp from the origin (Fig 4D). After loading the MCMs specifically at the origin (Fig S2), firing factors were added to form and activate CMG. Then, MseI restriction enzyme was added at indicated times for 3 minutes to cleave double-stranded DNA. The amount of unwound DNA is then measure by qPCR with primers flanking each of the cassettes. Using this assay, we found that ssDNA accumulated with time at each of the MseI sites, with a delay for distant sites from the origin reflecting time before CMG reached these sites (Fig 4E). We extracted from this data a rate of CMG helicase activity of ~79 bp/min. When we included Mrc1 in the reactions, ssDNA accumulated faster reflecting a CMG helicase rate of ~135 bp/min (Fig 4F). This data shows that Mrc1 can directly increase the rate of CMG helicase unwinding. When we incubated Mrc1 with Rad53 prior to addition to the helicase reaction, ssDNA accumulated at a rate similar to the -Mrc1 reactions (Fig 4G), indicating that Rad53 inhibits Mrc1's ability to stimulate the CMG helicase.

Identification of Rad53 phosphorylation sites in Mrc1

To understand how Rad53 regulates replication *in vitro* and *in vivo*, we undertook a mutational analysis of Mrc1 phosphorylation sites. The mutant Mrc1^{17AQ} protein, which cannot be phosphorylated by Mec1 (Osborn and Elledge, 2003), supported normal replication speed and was inhibited by Rad53 just as the wild-type Mrc1 indicating that the

bioRxiv preprint doi: https://doi.org/10.1101/2021.04.09.439171; this version posted April 10, 2021. The copyright holder for this preprint (which was not certified by peer review) is the author/funder, who has granted bioRxiv a license to display the preprint in perpetuity. It is made available under aCC-BY 4.0 International license.

Rad53 phosphorylation sites regulating Mrc1 activity in fork rate do not overlap the Mrc1 phosphorylation sites involved in signal transduction from Mec1 (Fig 5A). We note that the mobility of the Mrc1^{17AQ} protein in SDS-PAGE was not reduced after incubation with Rad53 (Fig 5C), suggesting that Rad53 can phosphorylate at least one of these 17 S/T-Q sites despite the site/s not being relevant for Rad53-dependent inhibition.

Deletion of the C-terminus of Mrc1, which has been implicated in regulating S-phase progression *in vivo*, slowed replication rate *in vitro*, and was not further inhibited by incubation with Rad53 (Fig 5B). Furthermore, the mobility of the Mrc1 truncation mutant was not reduced in SDS-PAGE after incubation with Rad53 (Fig 5C). These results suggest that the C-terminal region of Mrc1 is important for its function in regulating fork rate, and key Rad53 phosphorylation sites regulating this function may lie in this region.

Rad53 phosphorylation sites cannot be reliably predicted by primary amino acid sequence, so we took three unbiased approaches to identify the sites in Mrc1 that can be phosphorylated by Rad53 *in vitro*. First, we expressed and purified five overlapping protein fragments of Mrc1 and incubated each *in vitro* with Rad53 and γ^{32}P-ATP. As shown in Figure 5D, the fragment containing the last 228 amino acids of Mrc1, which includes the region required for fork rate stimulation (Fig 5A), was the best substrate for Rad53 *in vitro*. Second, we incubated Rad53 and γ^{32}P-ATP with a peptide array on which the entire Mrc1 protein sequence was 'printed' as overlapping 20-mer peptides (Fig S3A). Many of the peptides that were phosphorylated by Rad53 in this experiment also mapped to the C-terminus of Mrc1. Lastly, we used mass spectrometry to identify amino acids specifically phosphorylated by Rad53 (Fig S3B). Consistent with the peptide array and fragment analysis, many of the phosphorylated residues were in the C-terminus of Mrc1.

We used this information to generate a non-phosphorylatable Mrc1 mutant in which serine and threonine residues were changed to alanine: such a mutant should promote faster replication after incubation with Rad53 than wild type Mrc1. As shown in Figure 5E, we were able to generate mutants (Mrc1^{14A} and Mrc1^{19A}) that indeed exhibited faster

bioRxiv preprint doi: https://doi.org/10.1101/2021.04.09.439171; this version posted April 10, 2021. The copyright holder for this preprint (which was not certified by peer review) is the author/funder, who has granted bioRxiv a license to display the preprint in perpetuity. It is made available under aCC-BY 4.0 International license.

replication than wild type Mrc1 after Rad53 phosphorylation (compare lanes 2, 4 and 6). Unfortunately, these mutants — especially Mrc1^{19A} — did not stimulate replication to the rate of unphosphorylated wild-type Mrc1 (compare lanes 1, 4, and 6). This is likely due, in part, to the fact that these mutants exhibited defects in promoting faster replication in the absence of Rad53 indicating that they are not completely functional (compare lanes 1, 3, and 5). Moreover, even Mrc1^{19A} was still inhibited slightly by incubation with Rad53 (compare lanes 5 and 6), suggesting that additional sites not mutated in this construct can still be phosphorylated by Rad53 and inhibit Mrc1 function. Another mutant, Mrc1^{41A} in which all the serines and threonines within the fragment 5 of Figure 5D were mutated to alanines was even more defective than the other mutants in the absence of Rad53 but was not further inhibited by Rad53 (Fig S3C). Thus, we were unable to generate an Mrc1 mutant with wild type function when unphosphorylated and completely resistant to inhibition by Rad53 phosphorylation.

Mrc1^{8D} slows fork rate in vitro and partially rescues rad53 mutant in vivo

As an alternative approach, we generated an Mrc1 mutant in which potential phosphorylation sites were replaced with aspartate, mimicking the negative charge of phosphate: such a mutant is predicted be unable to promote faster replication even in the absence of Rad53. Indeed, a mutant in which 8 serine/threonine Rad53 phosphorylation sites were changed to aspartate (Mrc1^{8D}) was unable to stimulate replication even in the absence of Rad53 (Fig 6A). These 8 sites are a subset of the residues mutated in Mrc1^{14A} mutant that still retains near wild-type activity when not incubated with Rad53 (Figure 6A). This suggests that the inactivation seen in Mrc1^{8D} is not simply a consequence of changing essential serine or threonine residues.

Cells harbouring *MRC1^{8D}* as the only copy of *MRC1* activated Rad53, evidenced by Rad53 hyperphosphorylation, at the same time and to the same extent as *MRC1^{+}* cells after release from a G1 arrest into hydroxyurea, whilst *mrc1*Δ cells exhibited a reduced and delayed Rad53 activation (Fig 6B), consistent with previously published results (Alcasabas

bioRxiv preprint doi: https://doi.org/10.1101/2021.04.09.439171; this version posted April 10, 2021. The copyright holder for this preprint (which was not certified by peer review) is the author/funder, who has granted bioRxiv a license to display the preprint in perpetuity. It is made available under aCC-BY 4.0 International license.

et al., 2001). To rule out any contribution of the other mediator in Rad53 activation, Rad9, we repeated this experiment with strains in which *RAD9* was also deleted. As shown in Figure 6C, the *MRC1*^{8D} mutant supported Rad53 phosphorylation at the same time and to the same extent as wild type *MRC1*, even in the *rad9*Δ background (compare lanes 2-5, with lanes 7-10), whilst the *mrc1*Δ, *rad9*Δ double mutant was completely defective in Rad53 phosphorylation (lanes 12-15). *mrc1Δ rad9Δ* mutants are inviable (Alcasabas et al., 2001) and in this experiment were maintained by deletion of *SML1*; however, the *MRC1*^{8D} *rad9Δ* double mutants were viable without deletion of *SML1*. Taken together, these results indicate that Mrc1^{8D} can still signal from stalled replication forks, suggesting that the protein is stable *in vivo* (also seen in the Mrc1 immunoblots in Figure 6B,C) and maintains at least some interactions with the replisome.

If one of the functions of Rad53 is to slow replication after replication stress, then the *MRC1*^{8D} mutant might make *rad53Δ sml1Δ* cells more resistant to replication stress. Indeed, *MRC1*^{8D} *rad53Δ sml1Δ* cells showed some improvement in survival, compared to *rad53Δ sml1Δ* cells when chronically exposed to low concentrations of either HU (2 mM) or MMS (0.006%), though they did not promote additional survival to higher concentrations (8 mM HU and 0.01% MMS) (Fig 6D). Similar results were obtained with 2 freshly germinated spores of each genotype (Fig S4) arguing that the suppression seen was not a result of suppressor mutations, which accumulate readily in *rad53Δ sml1Δ* cells (Gómez-González et al., 2019). Figure 6E shows that *MRC1*^{8D} also promoted increased survival to acute exposure to higher concentration of MMS (0.02%) relative to *MRC1* wild type cells (Fig 6E). These data show that *MRC1*^{8D} can partially rescue the sensitivity of *rad53Δ sml1Δ* cells in response to chronic and acute replication stress, suggesting that slowing replication forks may be part of Rad53's role in protecting replication forks during the replication checkpoint.

Discussion

Our results show that, in addition to its role in checkpoint activation upstream of Rad53, Mrc1 also has a role downstream of the checkpoint, as a substrate of Rad53.

bioRxiv preprint doi: https://doi.org/10.1101/2021.04.09.439171; this version posted April 10, 2021. The copyright holder for this preprint (which was not certified by peer review) is the author/funder, who has granted bioRxiv a license to display the preprint in perpetuity. It is made available under aCC-BY 4.0 International license.

Phosphorylation of Mrc1 by Rad53 prevents Mrc1-dependent stimulation of CMG unwinding, leading to a reduced replication fork rate. We suggest that linking these two roles could allow Rad53 to slow replication speed specifically at a stressed or damaged fork, and, therefore, act efficiently at stochastic fork stalling events without initiating a global checkpoint response. But under more severe replication stress, where more Rad53 is active, Rad53 could phosphorylate Mrc1 at all forks to slow replication globally.

Using a novel assay to measure DNA unwinding activity, we found that unwinding by CMG is not very synchronous, as evidenced by shallow unwinding curves. Moreover, sites as close as 1 kb from the origin were not completely unwound after 50 min. In the presence of Mrc1, unwinding was faster and the curves were steeper, suggesting more synchronous unwinding leading to even the site 2 kb from the origin approaching 100% unwinding by 30 min. In single molecule experiments, CMG frequently paused and backtracked while unwinding DNA (Burnham et al., 2019). The ability to backtrack is thought to release CMG from a non-productive DNA duplex-engaged state in which duplex DNA enters the central CMG channel (Kose et al., 2020). Stochastic entry into this state may underlie the asynchronous unwinding curves in our assay, and Mrc1 could stimulate unwinding either by preventing CMG entry into the duplex-engaged state or by promoting its reversal. Regardless, it is interesting to consider that, by inhibiting Mrc1 and allowing CMG to either backtrack or engage the duplex, Rad53 may also contribute to replication fork repair or restart.

A recent structure of CMG bound to M/C/T suggests the C-terminus of Mrc1, containing the majority of its Rad53 phosphorylation sites, may contact Cdc45 and Mcm2 (Baretić et al., 2020). Other work has suggested an interaction with the non-catalytic domain of Polε (Lou et al., 2008). It would be interesting to understand how these interactions may drive Mrc1's stimulation of CMG activity and how phosphorylation modulates them. The $Mrc1^{8D}$ mutant showed normal checkpoint activation supporting the idea that it remains bound to replication forks. However, we note that Rad53 can target more than these 8 sites

bioRxiv preprint doi: https://doi.org/10.1101/2021.04.09.439171; this version posted April 10, 2021. The copyright holder for this preprint (which was not certified by peer review) is the author/funder, who has granted bioRxiv a license to display the preprint in perpetuity. It is made available under aCC-BY 4.0 International license.

and full phosphorylation may affect more functions and protein-protein interactions than those disrupted in the Mrc1^{8D} mutant.

Previous work using chromatin immunoprecipitation showed that CMG components moved further away from DNA replication in *mrc1*Δ cells treated with hydroxyurea, suggesting that Mrc1 has some role in restraining CMG at stalled forks (Katou et al., 2003). Superficially, this appears inconsistent with our results: loss of functional Mrc1 might be predicted to lead to slower CMG unwinding, and, therefore, less distance between CMG and DNA replication. However, our results, along with other previous work, suggest an explanation for this. In *mrc1*Δ cells, Rad53 activation is significantly delayed in hydroxyurea (Bacal et al., 2018; Osborn and Elledge, 2003). We suggest that during this delay, unphosphorylated Mcm10 continues to drive CMG progression, unwinding further from the stalled DNA synthesis; in wild type cells on the other hand, rapid Rad53 activation would inactivate both Mrc1 and Mcm10 leading to more rapid slowing of CMG. Why the cell utilises two targets to regulate fork progression is unclear, and further work is required to understand this.

Studies in mammalian cells have shown that replication forks are slowed down globally in response to replication checkpoint activation (Mutreja et al., 2018; Seiler et al., 2007). It would be interesting to explore whether Claspin, the mammalian homolog of Mrc1, or Mcm10 might be involved in this process during replication stress.

Experimental Procedures

Details of protein purification, yeast strain construction, and CMG helicase assay template are provided in the Supplemental Material.

Replication reactions

Replication reactions were essentially performed as in (Yeeles et al., 2017). Reaction buffer contained: 25 mM HEPES-KOH (pH 7.6), 100 mM potassium glutamate or sodium

bioRxiv preprint doi: https://doi.org/10.1101/2021.04.09.439171; this version posted April 10, 2021. The copyright holder for this preprint (which was not certified by peer review) is the author/funder, who has granted bioRxiv a license to display the preprint in perpetuity. It is made available under aCC-BY 4.0 International license.

acetate, 10 mM magnesium acetate, 2 mM DTT, 0.02% NP-40-S, and 5 mM ATP. Experiments were all performed in a thermomixer at 30°C and 1250 rpm. For experiments where proteins were preincubated with Rad53, samples were incubated with 5 mM ATP in reaction buffer for 15-30 min. MCM loading was performed in a master mix of 5 ul per sample with 40 nM ORC, 40 nM Cdc6, and 60 nM MCM-Cdt1 on 4 nM of 10.6 kb plasmid DNA with ARS1 origin. After 20 min, DDK was added to 40-50 nM and further incubated for 10 min. The reaction volume was then doubled with a protein mix and nucleotide mix to give the final concentration of: 20-80 nM Cdc45, 30 nM Dpb11, 20 nM Polε, 20 nM GINS, 15-20 nM CDK, 100 nM RPA, 20 nM Ctf4, 10 nM TopoI, 20 nM Csm3/Tof1, 20 nM Mrc1, 20-60 nM Polα, 20-25 nM Sld3/7, 20 nM Mcm10, 20-50nM Sld2, 200 μM CTP, 200 μM GTP, 200 μM UTP, 80 μM dCTP, 80 μM dGTP, 80 μM dTTP, 80 μM dATP, and 33-50 nM α^{32}P-dCTP. In Figure 4C, 20 nM PCNA, 20 nM RFC, and 20 nM Polδ, were also added in the last step. Reactions were then stopped by the addition of EDTA, processed over Illustra MicroSpin G-50 columns, separated on alkaline agarose gels, fixed in 5% trichloroacetic acid, dried, exposed to phosphor screens, and scanned using a Typhoon phosphorimager.

Four-step replication reactions (Figure 2A, 3A, and 3B) were modified from the three-step reactions above. Following DDK incubation, firing factors were added for 10 min prior to the addition of the remaining proteins and nucleotide mix.

Quantification of signal was performed using FIJI software. Image signal was linearised with “linearise gel data” plug-in. Distance was then calibrated to base pair length using the base pair ladder with an exponential fit. Each lane was fit with a smooth line using Prism 8, then the leading fork length was defined as the position where the signal was 20% the maximum signal of the lane.

In vitro kinase assays

For Figure 1A, 1C, 2C, 3C, and 5C, Rad53 was incubated at equimolar ratio to target protein with 5 mM ATP for 15 min prior to separation on SDS-PAGE and coomassie stain. For Figure 5D, Rad53 was incubated with target protein with 0.2 mM ATP and 0.2 μCi/μl

bioRxiv preprint doi: https://doi.org/10.1101/2021.04.09.439171; this version posted April 10, 2021. The copyright holder for this preprint (which was not certified by peer review) is the author/funder, who has granted bioRxiv a license to display the preprint in perpetuity. It is made available under aCC-BY 4.0 International license.

γ^{32}P-ATP for 15 min, processed over Illustra MicroSpin G-50 columns, separated on SDS-PAGE, coomassie stained, dried, exposed to phosphor screens, and scanned using a Typhoon phosphorimager.

Peptide array

Peptide arrays were synthesised on an Intavis ResPep SLi automated synthesiser (Intavis Bioanalytical Instruments AG, Cologne, Germany). The peptides were synthesised using FMOC for temporary α-amino group protection. Protecting groups used were Pbf for arginine, OtBu for glutamic acid and aspartic acid, Trt for asparagine, glutamine, histidine, and cysteine, tBu for serine, threonine and tyrosine, and Boc for lysine and tryptophan. Each amino acid was coupled by activating its carboxylic acid group with DIC in the presence of HOBT. Individual aliquots of amino acids were spotted on to a cellulose membrane which has been derivatised to have 8 to 10 ethylene glycol spacers between the cellulose and an amino group. Synthesis was accomplished by cycles of coupling of amino acids, washing then removal of the temporary α-amino protecting group by piperidine followed by more washing. Once the required number of cycles of coupling and deprotection and washing had been completed, the membranes were treated with a solution of 20 ml containing 95% TFA, 3% TIS, and 2% water for 4 h. Following this treatment, membranes were washed 4 times with DCM, 4 times with ethanol, and twice with water to remove side chain protecting groups and TFA salts and once again with ethanol for easier drying. Just prior to kinase assay, membranes were washed extensively in reaction buffer, then incubated with 80 nM Rad53, 10 μM ATP, and 0.02 μCi/μl γ^{32}P-ATP. Membranes were then washed with 1 M NaCl, 1% SDS, and 0.5% phosphoric acid prior to exposure to phosphor screens, and scanned using a Typhoon phosphorimager.

CMG helicase assay

The CMG helicase assays were performed with a 5 kb template containing an efficient artificial origin (Coster and Diffley, 2017) and cassettes of 4 MseI restriction cleavage sites (see Supplemental Experimental Procedures), which was linearised with

bioRxiv preprint doi: https://doi.org/10.1101/2021.04.09.439171; this version posted April 10, 2021. The copyright holder for this preprint (which was not certified by peer review) is the author/funder, who has granted bioRxiv a license to display the preprint in perpetuity. It is made available under aCC-BY 4.0 International license.

ScaI. MCM loading specifically at the origin was done as follows (and visualised with replication reaction in Fig S2): 5 min incubation of 10 nM DNA, 40 nM Orc, 5 mM ATP, 80 mM NaCl, in replication buffer at 30C and 1250 rpm. Then 40 nM Cdc6 and 60 nM MCM-Cdt1 are added for an additional 10 min followed by passing over a G-50 illustra micro-spin column pre-equilibrated in replication buffer to remove NaCl. ATP and 50 nM DDK are then added for 10 min, then the reaction volume is doubled with a final concentration of: 40-80 nM Cdc45, 30 nM Dpb11, 20 nM Polε^{exo-} (D290A, E292A), 20 nM GINS, 15 nM CDK, 20 nM Csm3/Tof1, 20 nM Mrc1, 20-30 nM Sld3/7, 20 nM Mcm10, 20-50 nM Sld2, and 350 nM RPA. At each time point, 2.5 µl of reaction was added to a tube containing 5 µl replication buffer and 1 µl MseI (NEB) for 3 min, and then the reaction was quenched with the addition of EDTA. Samples were then deproteinated with SDS and proteinase K followed by column clean-up (QIAquick PCR purification kit) according to manufacturer's instructions. The final elution was done with 300 µl 10 mM Tris pH 8. Then qPCR was performed in triplicate using 4 µl sample in 8-9 µl reaction with FastStart Universal SYBR Green Master Mix (Roche) and primers flanking each MseI cassette (Table S3).

Western Blot

Log-phase yeast cultures in YPD were diluted to OD600 0.5 and arrested with 20 ug/ml of alpha-factor for 2-3 h at 25C. Cells were washed two times with YPD and then resuspended in YPD + 200 mM hydroxyurea. Cells were then harvested at the indicated times, and protein was extracted with 10% trichloroacetic acid. Extracts were then processed by 3-8% Tris-acetate SDS-PAGE, transferred to nitrocellulose, and immunoblotted with anti-Flag (M2 mouse monoclonal) and anti-Rad53 (Abcam, ab104232, rabbit polyclonal) antibodies.

References

Abd Wahab, S., and Remus, D. (2020). Antagonistic control of DDK binding to licensed replication origins by Mcm2 and Rad53. Elife *9*, 1–28.

Alcasabas, A.A., Osborn, A.J., Bachant, J., Hu, F., Werler, P.J.H., Bousset, K., Furuya, K., Diffley, J.F.X., Carr, A.M., and Elledge, S.J. (2001). Mrc1 transduces signals of DNA replication stress to activate Rad53. Nat. Cell Biol. *3*, 958–965.

Bacal, J., Moriel-Carretero, M., Pardo, B., Barthe, A., Sharma, S., Chabes, A., Lengronne,

bioRxiv preprint doi: https://doi.org/10.1101/2021.04.09.439171; this version posted April 10, 2021. The copyright holder for this preprint (which was not certified by peer review) is the author/funder, who has granted bioRxiv a license to display the preprint in perpetuity. It is made available under aCC-BY 4.0 International license.

A., and Pasero, P. (2018). Mrc1 and Rad9 cooperate to regulate initiation and elongation of DNA replication in response to DNA damage. EMBO J. *37*, e99319.

Bando, M., Katou, Y., Komata, M., Tanaka, H., Itoh, T., Sutani, T., and Shirahige, K. (2009). Csm3, Tof1, and Mrc1 form a heterotrimeric mediator complex that associates with DNA replication forks. J. Biol. Chem. *284*, 34355–34365.

Baretić, D., Jenkyn-Bedford, M., Aria, V., Cannone, G., Skehel, M., and Yeeles, J.T.P. (2020). Cryo-EM Structure of the Fork Protection Complex Bound to CMG at a Replication Fork. Mol. Cell *78*, 926-940.e13.

Bastos de Oliveira, F.M., Harris, M.R., Brazauskas, P., de Bruin, R.A.M., and Smolka, M.B. (2012). Linking DNA replication checkpoint to MBF cell-cycle transcription reveals a distinct class of G1/S genes. EMBO J. *31*, 1798–1810.

Burnham, D.R., Kose, H.B., Hoyle, R.B., and Yardimci, H. (2019). The mechanism of DNA unwinding by the eukaryotic replicative helicase. Nat. Commun. *10*, 2159.

Coster, G., and Diffley, J.F.X. (2017). Bidirectional eukaryotic DNA replication is established by quasi-symmetrical helicase loading. Science *357*, 314–318.

Deegan, T.D., Yeeles, J.T., and Diffley, J.F. (2016). Phosphopeptide binding by Sld3 links Dbf4-dependent kinase to MCM replicative helicase activation. EMBO J. *35*, 961–973.

Devbhandari, S., and Remus, D. (2020). Rad53 limits CMG helicase uncoupling from DNA synthesis at replication forks. Nat. Struct. Mol. Biol. *27*, 461–471.

Francis, L.I., Randell, J.C.W., Takara, T.J., Uchima, L., and Bell, S.P. (2009). Incorporation into the prereplicative complex activates the Mcm2 – 7 helicase for Cdc7 – Dbf4 phosphorylation. Genes Dev. *23*, 643–654.

Gambus, A., Jones, R.C., Sanchez-Diaz, A., Kanemaki, M., van Deursen, F., Edmondson, R.D., and Labib, K. (2006). GINS maintains association of Cdc45 with MCM in replisome progression complexes at eukaryotic DNA replication forks. Nat. Cell Biol. *8*, 358–366.

Gilbert, C.S., Green, C.M., and Lowndes, N.F. (2001). Budding Yeast Rad9 Is an ATP-Dependent Rad53 Activating Machine. Mol. Cell *8*, 129–136.

Gómez-González, B., Patel, H., Early, A., and Diffley, J.F.X. (2019). Rpd3L Contributes to the DNA Damage Sensitivity of Saccharomyces cerevisiae Checkpoint Mutants. Genetics *211*, 503–513.

Goswami, P., Abid Ali, F., Douglas, M.E., Locke, J., Purkiss, A., Janska, A., Eickhoff, P., Early, A., Nans, A., Cheung, A.M.C., et al. (2018). Structure of DNA-CMG-Pol epsilon elucidates the roles of the non-catalytic polymerase modules in the eukaryotic replisome. Nat. Commun. *9*, 5061.

Katou, Y., Kanoh, Y., Bando, M., Noguchi, H., Tanaka, H., Ashikari, T., Sugimoto, K., and Shirahige, K. (2003). S-phase checkpoint proteins Tof1 and Mrc1 form a stable replication-pausing complex. Nature *424*, 1078–1083.

Kihara, M., Nakai, W., Asano, S., Suzuki, A., Kitada, K., Kawasaki, Y., Johnston, L.H., and Sugino, A. (2000). Characterization of the Yeast Cdc7p/Dbf4p Complex Purified from Insect Cells. J. Biol. Chem. *275*, 35051–35062.

Komata, M., Bando, M., Araki, H., and Shirahige, K. (2009). The Direct Binding of Mrc1, a Checkpoint Mediator, to Mcm6, a Replication Helicase, Is Essential for the Replication Checkpoint against Methyl Methanesulfonate-Induced Stress. Mol. Cell. Biol. *29*, 5008–5019.

Kose, H.B., Xie, S., Cameron, G., Strycharska, M.S., and Yardimci, H. (2020). Duplex DNA engagement and RPA oppositely regulate the DNA-unwinding rate of CMG helicase. Nat. Commun. *11*, 1–15.

bioRxiv preprint doi: https://doi.org/10.1101/2021.04.09.439171; this version posted April 10, 2021. The copyright holder for this preprint (which was not certified by peer review) is the author/funder, who has granted bioRxiv a license to display the preprint in perpetuity. It is made available under aCC-BY 4.0 International license.

Krishnan, V., Nirantar, S., Crasta, K., Cheng, A.Y.H., and Surana, U. (2004). DNA Replication Checkpoint Prevents Precocious Chromosome Segregation by Regulating Spindle Behavior. Mol. Cell *16*, 687–700.

Kumar, S., and Huberman, J.A. (2009). Checkpoint-Dependent Regulation of Origin Firing and Replication Fork Movement in Response to DNA Damage in Fission Yeast. Mol. Cell. Biol. *29*, 602–611.

Langston, L.D., Mayle, R., Schauer, G.D., Yurieva, O., Zhang, D., Yao, N.Y., Georgescu, R.E., and O'Donnell, M.E. (2017). Mcm10 promotes rapid isomerization of CMG-DNA for replisome bypass of lagging strand DNA blocks. Elife *6*, 1–21.

Lewis, J.S., Spenkelink, L.M., Schauer, G.D., Hill, F.R., Georgescu, R.E., O'Donnell, M.E., and van Oijen, A.M. (2017). Single-molecule visualization of Saccharomyces cerevisiae leading-strand synthesis reveals dynamic interaction between MTC and the replisome. Proc. Natl. Acad. Sci. *114*, 10630–10635.

Lõoke, M., Maloney, M.F., and Bell, S.P. (2017). Mcm10 regulates DNA replication elongation by stimulating the CMG replicative helicase. 291–305.

Lopes, M., Cotta-Ramusino, C., Pellicioli, A., Liberi, G., Plevani, P., Muzi-Falconi, M., Newlon, C.S., and Foiani, M. (2001). The DNA replication checkpoint response stabilizes stalled replication forks. Nature *412*, 557–561.

Lou, H., Komata, M., Katou, Y., Guan, Z., Reis, C.C., Budd, M., Shirahige, K., and Campbell, J.L. (2008). Mrc1 and DNA Polymerase ε Function Together in Linking DNA Replication and the S Phase Checkpoint. Mol. Cell *32*, 106–117.

Mutreja, K., Krietsch, J., Hess, J., Ursich, S., Berti, M., Roessler, F.K., Zellweger, R., Patra, M., Gasser, G., and Lopes, M. (2018). ATR-Mediated Global Fork Slowing and Reversal Assist Fork Traverse and Prevent Chromosomal Breakage at DNA Interstrand Cross-Links. Cell Rep. *24*, 2629-2642.e5.

Naylor, M.L., Li, J. -m., Osborn, A.J., and Elledge, S.J. (2009). Mrc1 phosphorylation in response to DNA replication stress is required for Mec1 accumulation at the stalled fork. Proc. Natl. Acad. Sci. *106*, 12765–12770.

Osborn, A.J., and Elledge, S.J. (2003). Mrc1 is a replication fork component whose phosphorylation in response to DNA replication stress activates Rad53. Genes Dev. *17*, 1755–1767.

Pardo, B., Crabbé, L., and Pasero, P. (2017). Signaling pathways of replication stress in yeast. FEMS Yeast Res. *17*, fow101.

Paulovich, A.G., and Hartwell, L.H. (1995). A checkpoint regulates the rate of progression through S phase in S. cerevisiae in Response to DNA damage. Cell *82*, 841–847.

Saldivar, J.C., Cortez, D., and Cimprich, K.A. (2017). The essential kinase ATR: Ensuring faithful duplication of a challenging genome. Nat. Rev. Mol. Cell Biol. *18*, 622–636.

Santocanale, C., and Diffley, J.F. (1998). A Mec1- and Rad53-dependent checkpoint controls late-firing origins of DNA replication. Nature *395*, 615–618.

Seiler, J.A., Conti, C., Syed, A., Aladjem, M.I., and Pommier, Y. (2007). The Intra-S-Phase Checkpoint Affects both DNA Replication Initiation and Elongation: Single-Cell and -DNA Fiber Analyses. Mol. Cell. Biol. *27*, 5806–5818.

Tercero, J.A., and Diffley, J.F.X. (2001). Regulation of DNA replication fork progression through damaged DNA by the Mec1/Rad53 checkpoint. Nature *412*, 553–557.

Tercero, J.A., Longhese, M.P., and Diffley, J.F.. (2003). A Central Role for DNA Replication Forks in Checkpoint Activation and Response. Mol. Cell *11*, 1323–1336.

Travesa, A., Kuo, D., De Bruin, R.A.M., Kalashnikova, T.I., Guaderrama, M., Thai, K.,

bioRxiv preprint doi: https://doi.org/10.1101/2021.04.09.439171; this version posted April 10, 2021. The copyright holder for this preprint (which was not certified by peer review) is the author/funder, who has granted bioRxiv a license to display the preprint in perpetuity. It is made available under aCC-BY 4.0 International license.

Aslanian, A., Smolka, M.B., Yates, J.R., Ideker, T., et al. (2012). DNA replication stress differentially regulates G1/S genes via Rad53-dependent inactivation of Nrm1. EMBO J. *31*, 1811–1822.

Yeeles, J.T.P., Deegan, T.D., Janska, A., Early, A., and Diffley, J.F.X. (2015). Regulated eukaryotic DNA replication origin firing with purified proteins. Nature *519*, 431–435.

Yeeles, J.T.P., Janska, A., Early, A., and Diffley, J.F.X. (2017). How the Eukaryotic Replisome Achieves Rapid and Efficient DNA Replication. Mol. Cell *65*, 105–116.

Zegerman, P., and Diffley, J.F.X. (2010). Checkpoint-dependent inhibition of DNA replication initiation by Sld3 and Dbf4 phosphorylation. Nature *467*, 474–478.

Zhang, Z.-X., Zhang, J., Cao, Q., Campbell, J.L., and Lou, H. (2018). The DNA Pol ϵ stimulatory activity of Mrc1 is modulated by phosphorylation. Cell Cycle *17*, 64–72.

Zhao, X., Muller, E.G.D., and Rothstein, R. (1998). A suppressor of two essential checkpoint genes identifies a novel protein that negatively affects dNTP pools. Mol. Cell *2*, 329–340.

Zhou, J.C., Janska, A., Goswami, P., Renault, L., Abid Ali, F., Kotecha, A., Diffley, J.F.X., and Costa, A. (2017). CMG–Pol epsilon dynamics suggests a mechanism for the establishment of leading-strand synthesis in the eukaryotic replisome. Proc. Natl. Acad. Sci. *114*, 4141–4146.

Zierhut, C., and Diffley, J.F.X. (2008). Break dosage, cell cycle stage and DNA replication influence DNA double strand break response. EMBO J. *27*, 1875–1885.

Author Contributions

AWM and JFXD conceived the study and interpreted experimental results. AWM purified proteins and carried out experiments. AWM wrote the manuscript with input from JFXD.

Acknowledgements

We thank A Alidoust, N Patel, and D Patel in the Structural Biology Laboratory for yeast protein expression. We thank D Joshi in the Peptide Chemistry Laboratory for generating the Mrc1 peptide arrays and D Frith in the Proteomics Laboratory for processing mass spectrometry samples. We thank V Posse for providing Mrc1^{17AQ} protein. We thank V Posse, A Bertolin, B Canal, and all members of the Diffley group for stimulating discussions and advice. This work was supported by the Francis Crick Institute, which receives its core funding from Cancer Research UK (FC001066), the UK Medical Research Council (FC001066), and the Wellcome Trust (FC001066). This work was also funded by an EMBO Long-Term Fellowship (ALTF 1259-2016 to AWM), Wellcome Trust Senior Investigator Awards (106252/Z/14/Z and 219527/Z/19/Z to JFXD), and a European Research Council

bioRxiv preprint doi: https://doi.org/10.1101/2021.04.09.439171; this version posted April 10, 2021. The copyright holder for this preprint (which was not certified by peer review) is the author/funder, who has granted bioRxiv a license to display the preprint in perpetuity. It is made available under aCC-BY 4.0 International license.

Advanced Grant (669424-CHROMOREP to JFXD). For the purpose of Open Access, the author has applied a CC BY public copyright licence to any Author Accepted Manuscript version arising from this submission.

bioRxiv preprint doi: https://doi.org/10.1101/2021.04.09.439171; this version posted April 10, 2021. The copyright holder for this preprint (which was not certified by peer review) is the author/funder, who has granted bioRxiv a license to display the preprint in perpetuity. It is made available under aCC-BY 4.0 International license.

Figure Legends

Figure 1

Rad53 inhibition of origin firing. A) DDK was incubated with Rad53 or Rad53^{KD} (K227A, K339A) for 15 min, separated by SDS-PAGE, and stained with coomassie. B) DDK was incubated with Rad53 for 15 min and then added to a standard 3-step in vitro replication reaction (see Experimental Procedures for more details). After 20 min, reactions were stopped with EDTA and products were separated on an alkaline agarose gel. C) Sld3/7 was incubated with Rad53 as in A). D) Sld3/7 was incubated with Rad53 and added to a replication reaction. In lane 4, Sld3/7 and Rad53 were incubated separately from each other prior to addition to the replication reaction, and in lane 5, ATP was omitted during the pre-incubation.

Figure 2

Rad53 inhibition of replication elongation via Mrc1. A) Elongation factors (here, defined as RPA, Ctf4, TopoI, Mrc1, Csm3/Tof1, Polα, and Mcm10) were pre-incubated with Rad53 prior to addition to a 4-step replication reaction that was stopped at the indicated timepoints. B) Leading fork lengths (see Experimental Procedures for quantification method) at each timepoint from A) with a linear fit. C) Mrc1 or Csm3/Tof1 were incubated with Rad53, separated by SDS-PAGE, and stained with coomassie. D) M/C/T or individual Mrc1 and Csm3/Tof1 were incubated with Rad53 prior to addition to a replication reaction. Reactions were stopped at 7 min (not completion).

Figure 3

Mrc1 phosphorylation is necessary for Rad53 dependent inhibition of elongation. A) Elongation factors were pre-incubated with Rad53 prior to addition to a 4-step replication reaction that was stopped at the indicated timepoints. Mrc1 was omitted from the pre-incubation step in lanes 7-9 and added separately. B) Reactions were performed as in A) except M/C/T was omitted from the pre-incubation with Rad53 and added separately as indicated. C) Mcm10 was incubated with Rad53, separated by SDS-PAGE, and stained with

bioRxiv preprint doi: https://doi.org/10.1101/2021.04.09.439171; this version posted April 10, 2021. The copyright holder for this preprint (which was not certified by peer review) is the author/funder, who has granted bioRxiv a license to display the preprint in perpetuity. It is made available under aCC-BY 4.0 International license.

coomassie. D) Mrc1 and Mcm10 were incubated with Rad53 prior to addition to a replication reaction (scheme to the left). Mrc1 was omitted from lane 4 and 5. Reactions were stopped at 7 min. E) Mcm10 was incubated with the indicated concentration of Rad53 prior to addition to a replication reaction in the presence of Mrc1.

Figure 4

Mrc1 regulation of replication rate. A) Mrc1 was omitted, incubated alone, or incubated with Rad53 prior to adding to a replication reaction. Reactions were stopped after 7 min. B) Reactions as in A) but using the catalytically-dead mutant (Polε$^{\Delta CAT}$) of Polε, and reactions were stopped at 10 min. C) Reactions as in A) but with Polε$^{\Delta CAT}$ and the addition of PCNA, RFC, and Polδ. D) Helicase assay scheme. After MCMs are loaded specifically at the origin, CMGs are activated and unwind DNA. At each timepoint, MseI is added to digest DNA that is double-stranded; MseI does not digest single-stranded, RPA-coated DNA. The reactions are then quenched, proteins removed, and qPCR is performed using primers flanking the MseI cleavage sites, which generate a signal from the unwound DNA. E) Timecourse of reactions depicted in D). Data is normalised to the amount of unwound DNA at the closest MseI site (0.2 kb from the origin) at the last timepoint (see Experimental Procedures for more detail). F) Reactions as in E) with the addition of Mrc1. D) Reactions as in E) where Mrc1 is incubated with Rad53.

Figure 5

Identification of Rad53-dependent phospho-sites on Mrc1. A) Mrc1^{17AQ} mutant was incubated with Rad53 prior to addition to in vitro replication for 7 min. B) C-terminal truncation of Mrc1 was incubated with Rad53 prior to addition to in vitro replication for 7 min. Note that all lanes were run on the same alkaline agarose gel, but other samples between lanes 2 and 3 were removed for clarity. C) Mrc1, Mrc1 truncation, and Mrc1^{17AQ} were incubated with Rad53 and separated by SDS-PAGE then stained with coomassie. D) Fragments of Mrc1 were incubated with Rad53, separated by SDS-PAGE, then subjected to

bioRxiv preprint doi: https://doi.org/10.1101/2021.04.09.439171; this version posted April 10, 2021. The copyright holder for this preprint (which was not certified by peer review) is the author/funder, who has granted bioRxiv a license to display the preprint in perpetuity. It is made available under aCC-BY 4.0 International license.

autoradiography. E) Mrc1, Mrc1^{14A}, and Mrc1^{19A} were incubated with Rad53 prior to addition to in vitro replication assay for 7 min.

Figure 6

Mrc1^{8D} slows fork rate in vitro and partially rescues *rad53Δ* sensitivity to replication stress. A) Mrc1 and Mrc1^{8D} were incubated with Rad53 prior to addition to replication reaction for 7 min. B) Cells harbouring *MRC1-3xFLAG* (yAWM336), *MRC1^{8D}-3xFLAG* (yAWM291), or *mrc1Δ* (yAWM217) were synchronised in G1 with α-factor then released into media with or without 200 mM hydroxyurea for the indicated timepoints. TCA lysates were then analysed by western blot with the indicated antibodies. C) Cells that contained *sml1Δ rad9Δ* in addition to *MRC1-3xFLAG* (yAWM346), *MRC1^{8D}-3xFLAG* (yAWM348), or *mrc1Δ* (yJT135) were treated as in B). D) Cells that contained *sml1Δ* as well as *MRC1-3xFLAG* (yAWM337), *MRC1^{8D}-3xFLAG* (yAWM292), *MRC1-3xFLAG* and *rad53Δ* (yAWM338), or *MRC1^{8D}-3xFLAG* and *rad53Δ* (yAWM293) were spotted as 1:10 serial dilutions onto YPD plates supplemented with the indicated drugs. E) Cells from D) were arrested in G1 with alpha-factor then released into media with or without 0.02% MMS for the indicated timepoints then plated on YPD plates.

bioRxiv preprint doi: https://doi.org/10.1101/2021.04.09.439171; this version posted April 10, 2021. The copyright holder for this preprint (which was not certified by peer review) is the author/funder, who has granted bioRxiv a license to display the preprint in perpetuity. It is made available under aCC-BY 4.0 International license.

Supplemental Material

Supplemental Figure S1

Rad53 phosphorylation of Sld3/7. A) Coomassie stained SDS-PAGE of Rad53 (shifted due to autophosphorylation during expression in bacteria (Gilbert et al., 2001)) and Rad53^{KD}. B) Replication reactions with Sld3/7 pre-incubated with Rad53 at varying concentrations.

Supplemental Figure S2

Origin-specific MCM loading conditions. Replication reactions using 10 nM of the 5 kb CMG helicase assay template (or a version without the ORC binding sites) using normal replication buffer or using the origin-specific loading conditions, which include 80 mM NaCl and processing over a G50 column. The template was linearised prior to the reaction with NheI leading to a 3.5 kb and 1.5 kb distance between the origin and the ends of the template. Note the smear of products centered at 2.5 kb from non-specific loading, which would produce leading strands that average half-template length.

Supplemental Figure S3

Identification of Rad53-dependent phospho-sites on Mrc1. A) Autoradiograph of peptide array of 20-mers scanning the Mrc1 peptide sequence after incubation with Rad53 and γ^{32}P-ATP. The asterisk (*) denotes the first 20-mer that contains an amino acid from fragment 5 of the fragment analysis experiment (Fig 5D). B) Sites identified by mass spectrometry. The gray highlighting indicates Mrc1 peptides that were detected, and red indicates serines and threonines that were specifically phosphorylated in the Rad53 sample (see Supplemental Table S5). Note the last 7 red amino acids fall within fragment 5 of the fragment analysis (Fig 5D). C) Mrc1 or Mrc1^{41A} were incubated with Rad53 prior to addition to a replication reaction for 7 min.

Supplemental Figure S4

Just after separating tetrad spores, 2 strains of each of the indicated genotype (with *sml1Δ*) were identified, grown for 6 h, and then spotted in 1:10 serial dilutions on the indicated

bioRxiv preprint doi: https://doi.org/10.1101/2021.04.09.439171; this version posted April 10, 2021. The copyright holder for this preprint (which was not certified by peer review) is the author/funder, who has granted bioRxiv a license to display the preprint in perpetuity. It is made available under aCC-BY 4.0 International license.

plates. Note the similar phenotype between the first four rows indicating *MRC1-3xFLAG* does not alter phenotype.

Supplemental Table S1. Yeast strains generated in this study.

Strain	Genotype (all in W303 background)
yVP8	*MAT***a** *bar1::hyg*^{R} *pep4::kan*^{R} *his3:pRS303-Gal1*$_{prom}$*-3xFLAG-DPB11:HIS3*
yVP7	*MAT***a** *bar1::hyg*^{R} *pep4::kan*^{R} *his3:pRS303-Gal1*$_{prom}$*-MRC1*^{17AQ}*-3xFLAG:HIS3*
yAWM106	*MAT***a** *bar1::hyg*^{R} *pep4::kan*^{R} *his3:pRS303-Gal1*$_{prom}$*-MRC1*$^{1-875}$*-3xFLAG:HIS3*
yAWM107	*MAT***a** *bar1::hyg*^{R} *pep4::kan*^{R} *his3:pRS303-Gal1*$_{prom}$*-MRC1*^{8D}*-3xFLAG:HIS3*
yAWM105	*MAT***a** *bar1::hyg*^{R} *pep4::kan*^{R} *his3:pRS303-Gal1*$_{prom}$*-MRC1*^{14A}*-3xFLAG:HIS3*
yAWM115	*MAT***a** *bar1::hyg*^{R} *pep4::kan*^{R} *his3:pRS303-Gal1*$_{prom}$*-MRC1*^{19A}*-3xFLAG:HIS3:NAT*
yAWM108	*MAT***a** *bar1::hyg*^{R} *pep4::kan*^{R} *his3:pRS303-Gal1*$_{prom}$*-MRC1*^{41A}*-3xFLAG:HIS3*
yAWM343	*MAT***a***/α* *Mrc1*^{8D}*-3xFLAG:nat*^{R}*/MRC1* *sml1::kan*^{R}*/SML1* *rad9::LEU2/RAD9*
yAWM337	*MAT***a** *MRC1-3xFLAG:nat*^{R} *sml1::kan*^{R}
yAWM292	*MAT***a** *MRC1*^{8D}*-3xFLAG:nat*^{R} *sml1::kan*^{R}
yAWM338	*MAT***a** *MRC1-3xFLAG:nat*^{R} *rad53::LEU2* *sml1::kan*^{R}
yAWM293	*MAT***a** *MRC1*^{8D}*-3xFLAG:nat*^{R} *rad53::LEU2* *sml1::kan*^{R}

bioRxiv preprint doi: https://doi.org/10.1101/2021.04.09.439171; this version posted April 10, 2021. The copyright holder for this preprint (which was not certified by peer review) is the author/funder, who has granted bioRxiv a license to display the preprint in perpetuity. It is made available under aCC-BY 4.0 International license.

yAWM336	*MAT***a** *MRC1-3xFLAG:nat^{R}*
yAWM291	*MAT***a** *MRC1^{8D}-3xFLAG:nat^{R}*
yAWM217	*MAT***a** *mrc1::kan^{R}*
yAWM346	*MAT***a** *MRC1-3xFLAG:nat^{R}* *rad9::LEU2* *sml1::kan^{R}*
yAWM348	*MAT***a** *MRC1^{8D}-3xFLAG:nat^{R}* *rad9::LEU2* *sml1::kan^{R}*
yJT135	*MAT***a** *sml1::URA3* *rad9::TRP1* *mrc1::HIS3*

Supplemental Table S2. DNA plasmids generated in this study.

Plasmid	**Description *see details in the construction notes**
pAWM7	pET21b-RAD53^{K227A,D339A}-6xHis
pAWM10	pET21b-MRC1$^{1-283}$-6xHis
pAWM11	pET21b-MRC1$^{110-430}$-6xHis
pAWM12	pET21b-MRC1$^{355-670}$-6xHis
pAWM13	pET21b-MRC1$^{555-900}$-6xHis
pAWM14	pET21b-MRC1$^{869-1096}$-6xHis
pAWM16	pRS303-GAL1$_{prom}$-MRC1-3xFLAG, GAL4
pVP14	pRS303-GAL1$_{prom}$-MRC1^{17AQ}-3xFLAG, GAL4
pAWM35	pRS303-GAL1$_{prom}$-MRC1$^{1-875}$-3xFLAG, GAL4
pAWM15	pRS303-GAL1$_{prom}$-MRC1^{14A}-3xFLAG, GAL4
pAWM25	pRS40N- MRC1^{19A}-3xFLAG (N-terminal truncation for integration)
pAWM18	pRS303-GAL1$_{prom}$-MRC1^{41A}-3xFLAG, GAL4
pAWM17	pRS303-GAL1$_{prom}$-MRC1^{8D}-3xFLAG, GAL4
pAWM48	pRS40N-MRC1-3xFLAG (N-terminal truncation for integration)
pAWM47	pRS40N-MRC1^{8D}-3xFLAG (N-terminal truncation for integration)
pAWM36	pBS-based template for CMG helicase assay
pAWM37	pBS-based template for CMG helicase assay (no origin)

Supplemental Table S3. Protein purification strategy.

Protein	**Purification strategy** (see (Deegan et al., 2016; Yeeles et al., 2015, 2017) for more details)
MCM-Cdt1	yeast expression, calmodulin pull-down, EGTA elution, gel filtration
Cdc6	bacterial expression, glutathione pull-down, precission protease elution, HTP column, dialysis
ORC	yeast expression, calmodulin pull-down, EGTA elution, gel filtration

bioRxiv preprint doi: https://doi.org/10.1101/2021.04.09.439171; this version posted April 10, 2021. The copyright holder for this preprint (which was not certified by peer review) is the author/funder, who has granted bioRxiv a license to display the preprint in perpetuity. It is made available under aCC-BY 4.0 International license.

DDK	yeast expression, calmodulin pull-down, EGTA elution, gel filtration
Rad53	bacterial expression, Ni-NTA pull-down, imidazole elution, gel filtration
Mrc1	yeast expression, Flag pull-down, flag peptide elution, MonoQ, dialysis
Cdc45	yeast expression, Flag pull-down, flag peptide elution, HTP column, dialysis
Dpb11	yeast expression, Flag pull-down, flag peptide elution, gel filtration
Polε and Polε^{exo-}	yeast expression, calmodulin pull-down, EGTA elution, heparin column, gel filtration
Polε$^{\Delta CAT}$	yeast expression, calmodulin pull-down, EGTA elution, MonoQ, gel filtration
GINS	bacterial expression, Ni-NTA pull-down, imidazole elution, MonoQ, gel filtration
CDK	yeast expression, calmodulin pull-down, TEV elution, Ni-NTA column, gel filtration
RPA	yeast expression, calmodulin pull-down, EGTA elution, heparin column, gel filtration
Ctf4	yeast expression, calmodulin pull-down, EGTA elution, MonoQ, gel filtration
TopoI	yeast expression, calmodulin pull-down, EGTA elution, gel filtration
Csm3/Tof1	yeast expression, calmodulin pull-down, TEV elution, gel filtration
Polα	yeast expression, calmodulin pull-down, EGTA elution, MonoQ, gel filtration
Sld3/7	yeast expression, IgG Sepharose 6 pull-down, TEV elution, Ni-NTA column, gel filtration
Mcm10	bacterial expression, Ni-NTA pull-down, imidazole elution, gel filtration
Sld2	yeast expression, ammonium sulphate precipitation, Flag pull-down, flag peptide elution, SP column, dialysis
RFC	yeast expression, calmodulin pull-down, EGTA elution, MonoS, gel filtration
PCNA	bacterial expression, ammonium sulphate precipitation, SP column, heparin column, DEAE column, MonoQ, gel filtration
Polδ	yeast expression, calmodulin pull-down, EGTA elution, heparin column, gel filtration

Supplemental Table S4. Primers used in CMG helicase assay.

site (distance from origin)	primer numbers	sequences
200 bp	AWM107 AWM109	CACTGCACCAAGGTAACACTC GAAGTCAGAGCTGGAGAATCCG
500 bp	AWM111 AWM112	CCCTACTTCAGCGCCATTCG TAACGGAAGCACCGAATCGT
1000 bp	AWM113 AWM115	CTCGTTGTGACGCCAATCAG ACATTGAGCCTACGCATCTGT
1500 bp	AWM78 AWM79	ACTACTGTCACTTCTGAGGGTTC CAGAGGGATGCGTAGTCGTG

bioRxiv preprint doi: https://doi.org/10.1101/2021.04.09.439171; this version posted April 10, 2021. The copyright holder for this preprint (which was not certified by peer review) is the author/funder, who has granted bioRxiv a license to display the preprint in perpetuity. It is made available under aCC-BY 4.0 International license.

2000 bp	AWM116 AWM117	CGGGGGAAGGAACTCTTGC AGGGGTCGTCAAGCAGAGAT
control site (not flanking MseI)	AWM84 AWM85	CTCTGCTTGACGACCCCTTG] TGTCCGTCCGAGAGCGATA

Supplemental Table S5. Mrc1 peptides detected by mass spectrometry.

Supplemental Experimental Procedures

Yeast and plasmid strain construction

RAD53^{K227A,K339A} was constructed by PCR with mutated oligos on pET21b-RAD53 (Gilbert et al., 2001). Mrc1 fragments were made by PCR from genomic DNA and cloned into pET21b vector with NheI and XhoI. pAWM16, pVP14, pAWM35, pAWM15, pAWM17, and pAWM18 were derived from the original plasmid yJY17 with the codon-optimised sequence of *MRC1* (Yeeles et al., 2017) and modified with Gibson assembly methods, and then transformed into the *his3* locus by cleaving with NheI. pAWM25 contained the C-terminal portion of MRC1^{19A} (starting from base pair 1395) and the 3xFLAG tag between the BamHI and NotI sites of pRS40N and then was cut with Blp1 to modify the already integrated codon-optimised MRC1 at the *his3* locus. pVP14 (MRC1^{17AQ}) contains all S/T residues followed by Q sites mutated to A as in (Osborn and Elledge, 2003). pAWM15 (MRC1^{14A}) contains the following mutations: S911A, S918A, S920A, T952A, S957A, T996A, T997A, S1006A, S1033A, T1036A, S1039A, S1040A, S1043A, T1045A. pAWM25 (MRC1^{19A}) contains the following mutations: T882A, S911A, S918A, S920A, S924A, T932A, T952A, S957A, S958A, T996A, S997A, S1006A, S1010A, S1033A, T1036A, S1039A, S1040A, S1043A, T1045A. pAWM18 (Mrc1^{41A}) contains the following mutations: T882A, S911A, S918A, S920A, S924A, T932A, S937A, T952A, S957A, S958A, S961A, T963A, S965A, T967A, S969A, T970A, T971A, S972A, T974A, T977A, T996A, S997A, S1006A, S1010A, S1013A, T1015A, T1027A, S1033A, T1036A, S1039A, S1040A, S1043A, T1045A, T1050A, T1060A, T1063A, T1079A, T1081A, S1083A, S1089A, S1093A. pAWM17 (Mrc1^{8D}) contains the following mutations: S911D, S918D, S920D, T952D, S957D, T996D, S997D, S1006D. pAWM47 and

bioRxiv preprint doi: https://doi.org/10.1101/2021.04.09.439171; this version posted April 10, 2021. The copyright holder for this preprint (which was not certified by peer review) is the author/funder, who has granted bioRxiv a license to display the preprint in perpetuity. It is made available under aCC-BY 4.0 International license.

pAWM48 contained base pairs 1424-3288 of MRC1 between XhoI and BamHI and 127 bp of the 3' UTR of MRC1 between BamHI and NotI. The 3xFLAG tag was added with flanking BamHI sites, and the plasmids were integrated into yeast after cutting with XbaI. The template used in the CMG helicase assay was made by modifying a plasmid with a pBlueScript vector and contained a synthetic origin with either two ORC binding sites 70 bp apart (pAWM36) or no ORC binding sites (pAWM37) (Coster and Diffley, 2017) and a synthetic fragment from GeneArt (Thermofisher) that contained the tandem MseI sites. See full pAWM36 plasmid sequence below.

CMG helicase assay template sequence (pAWM36)

AGTACTCAACCAAGTCATTCTGAGAATAGTGTATGCGGCGACCGAGTTGCTCTTGCCC
GGCGTCAATACGGGATAATACCGCGCCACATAGCAGGACTTTAAAAGTGCTCATCATTG
GAAAACGTTCTTCGGGGCGAAAACTCTCAAGGATCTTACCGCTGTTGAGATCCAGTTCG
ATGTAACCCACTCGTGCACCCAACTGATCTTCAGCATCTTTTACTTTCACCAGCGTTTCT
GGGTGAGCAAAAACAGGAAGGCAAAATGCCGCAAAAAAGGGAATAAGGGCGACACGG
AAATGTTGAATACTCATACTCTTCCTTTTTCAATATTATTGAAGCATTTATCAGGGTTATT
GTCTCATGAGCGGATACATATTTGAATGTATTTAGGGGAATAAACAAATAGGGGTTCCG
CGCACATTTCCCCGAAAAGTGCCACCTGACGTCTAAGAAACCATTATTATCATGACATT
GGCCTATAAAAATAGGCGTATCACGAGGCCCTTTCGTCTCGCGCGTTTCGGTGATGAC
GGTGAAAACCTCTGACACATGCAGCTCCCGGAGACGGTCACAGCTTGTCTGTAAGCGG
ATGCCGGGAGCAGACAAGCCCGTCAGGGCGCGTCAGCGGGTGTTGGCGGGTGTCGG
GGCTGGCTTAACTATGCGGCATCAGAGCAGATTGTACTGAGAGTGCACCATATGCGGT
GTGAAATACCGCACAGATGCGTAAGGAGAAAATACCGCATCAGGCGCCATTCGCCATT
CAGGCTGCGCAACTGTTGGGAAGGGCGATCGGTGCGGGCCTCTTCGCTATTACGCCA
GCTGGCGAAAGGGGGATGTGCTGCAAGGCGATTAAGTTGGGTAACGCCAGGGTTTTC
CCAGTCACGACGTTGTAAAACGACGGCCAGTGAATTCCTCGATTTTTTTATGTTTAGTTT
CGCGGACGACGGTTTCGAGGTGGCGGTCTGGACCACGCCGGAGAGCGTCGAAGCGG
AGGCGGTGTTCGCCGAGATCGGCTCGCGCAAAGCCGAGTTGAGCGAACTAAACATAAA
AATACAGCATCAGATGGTAGGCCTCCTGGCGCCGCACCGGCCTCAGCATCCGGTACCT
CAGCTGGCCACATCACTGTCTTTCTTATGACGGTACTACCGGTGTTCACTGCACCAAGG
TAACACTCATTAAATTAAGGTTAAATTAATCTACACAATTCTCTTTTGCTATTGGTACCGG
ATTCTCCAGCTCTGACTTCAGCGTCTCTGAAGGAATCTTTGCAGGTGCTTACGCTTACT
ACCTAAACTACAATGGTGTTGTCGCTACTAGTGCCGCTTCTTCAACCACTGGATCTGGT
CCTAGGGCTTCGGTCCGCCCCTACTTCAGCGCCATTCGCCATTCAGGCTGCGCAACTG
TTGGGAAGGGCGATCGGTGCGGGCCTCTTCGCTATTACGCCAGCTGGCGAAAGGGGG
ATGTGCTGCAATTCGGTTAAGTTAAGTTAAGGTTAAAGAAGCTAACGCCAGGGTTTTCC
CAGTCACGATTCGGTGCTTCCGTTACCGGTTCAACTGCTTCCACTTCATGGGCTACTTT
TTGGACCGGAACGGCTGGTACTATCGGCCTGGTATCATCCTTTACCGAAGCAACATCT
GTTTACACTACAACACTAGACCAAGCACAGTCGTAGTTTCTTGTTCAGAGATGACTCCA
ATGGTAACGTCTATACCATTACCACAATCATTAAGTTAAATTAAGTTAATCAAACCGTTC
CATGCTCATCCACTACCGCCACTATTACTTCTTGTGATGAAACTGGATGTCACGTTAGTA
CATCAACCGGTGCTGTTGTAACTGAAACCGTTTCTTCCAAGGCATACACAACTGCCAAA
GTAACTCGTTGTGACGCCAATCAGCTTGTCTGTAAGCGGATGCCGGGAGCAGACAAGC
CCGTCAGGGCGCGTCAGCGGGTGTTGGCGGGTGTCGGGGCATGGTTAAAGTTAACTT
AAATTAAGGTACGCGGCATCAGAGCAGATTGTACTGAGAGTGCACCATATGCGGTGTG
AAATACCGCACAGATGCGTAGGCTCAATGTAACTTAGCCACTGTCAATTGGGAATGTTC

bioRxiv preprint doi: https://doi.org/10.1101/2021.04.09.439171; this version posted April 10, 2021. The copyright holder for this preprint (which was not certified by peer review) is the author/funder, who has granted bioRxiv a license to display the preprint in perpetuity. It is made available under aCC-BY 4.0 International license.

CAGGGATTCATGGACAACAACTGCAACTGGAGTATCATACACCACTGTCACCGTAACCC
ACTGTGACGACAATGGCTGTAACACCAAGACTAAGCTCCTGAAGCTACCACCACAACTA
TCGCCCACCAGGACCACCGTCACCTTTAGTGATGACAATGAAGGTAAGACCTTGGGTG
AGTCTGGTCCAGCGGAGGGCCACTACTGTTTCTCCAAAGACATACACCACCGCTACTG
TTACTCAGGGGGATAAAAATGCCTGCCTCACCAAGACTGTCACTTCTGAATGTCCTGAA
GAAACTTCAGCAACTACTACTGTCACTTCTGAGGGTTCTAAAGCAACCTCATTGAGTCG
ACGCGGGGGCGACGATTAACCTTAACGTTAAGTTAAGCTAGCACGACTACGCATCCCT
CTGACTACTTCTCGGGGTGGGACTATACTGGTACCGATACGGGCTGTGATGACAACGA
TGTGTAGAACTGGGACAATCAGATCTGAGGCCCCTGAAGCCACAACGGGTACTGTTTC
TAACAACAGATACAACATGGAGGGCCAACATTGTCACAATAGAAGCTCCGCCAGAAACA
GTAGAAACTTCAGAAACCAGTGCTGCCCCTAAGGACATACACTACTGCCACTGGTTACT
CAATGGTTTAGAGGGTGGTTGCCACGTCAAGATAATCACCTCTAAAATACCTGAAGCTA
CTTCAACCGTCACGGGTGCTTCTCCAAAACGGCCTTACATAGCCGGATACAGTGACTTT
GACAGGTTTGCGGGGCACAGCAATGACTTGCATAGCTGCGTGCGGGGGAAGGAACTC
TTGCGTCTCACTGCCCGCTTTCCAGTCGGGAAACCTGTCGTGCCATTATGGTTAACTTA
AGTTAATTTAAGCTATCGGCCAACGCGCGGGGAGAGGCGGTTTGCGTATTGGGCGCTC
TTCCGCTTCCTCGCTCAGTGAGTATCTCTGCTTGACGACCCCTTGGCGCAGAGGTGCT
GGCCGCGTGCTAAGTTGAAGCGGCTGCACTGCTGCAAGGTCCGTCACGGAGGCGTCG
GACCGGCAGGAGCACTAGCCCATCGACCCGTACGGGAACACTCTATATCGCTCTCGGA
CGGACATTCTGGATCCTCTAGAGTCGACCTGCAGGCATGCAAGCTTGGCGTAATCATG
GTCATAGCTGTTTCCTGTGTGAAATTGTTATCCGCTCACAATTCCACACAACATACGAGC
CGGAAGCATAAAGTGTAAAGCCTGGGGTGCCTAATGAGTGAGCTAACTCACATTAATTG
CGTTGCGCTCACTGCCCGCTTTCCAGTCGGGAAACCTGTCGTGCCAGCTGCATTAATG
AATCGGCCAACGCGCGGGGAGAGGCGGTTTGCGTATTGGGCGCTCTTCCGCTTCCTC
GCTCACTGACTCGCTGCGCTCGGTCGTTCGGCTGCGGCGAGCGGTATCAGCTCACTC
AAAGGCGGTAATACGGTTATCCACAGAATCAGGGGATAACGCAGGAAAGAACATGTGA
GCAAAAGGCCAGCAAAAGGCCAGGAACCGTAAAAAGGCCGCGTTGCTGGCGTTTTTCC
ATAGGCTCCGCCCCCCTGACGAGCATCACAAAAATCGACGCTCAAGTCAGAGGTGGCG
AAACCCGACAGGACTATAAAGATACCAGGCGTTTCCCCCTGGAAGCTCCCTCGTGCGC
TCTCCTGTTCCGACCCTGCCGCTTACCGGATACCTGTCCGCCTTTCTCCCTTCGGGAA
GCGTGGCGCTTTCTCATAGCTCACGCTGTAGGTATCTCAGTTCGGTGTAGGTCGTTCG
CTCCAAGCTGGGCTGTGTGCACGAACCCCCCGTTCAGCCCGACCGCTGCGCCTTATCC
GGTAACTATCGTCTTGAGTCCAACCCGGTAAGACACGACTTATCGCCACTGGCAGCAG
CCACTGGTAACAGGATTAGCAGAGCGAGGTATGTAGGCGGTGCTACAGAGTTCTTGAA
GTGGTGGCCTAACTACGGCTACACTAGAAGAACAGTATTTGGTATCTGCGCTCTGCTGA
AGCCAGTTACCTTCGGAAAAAGAGTTGGTAGCTCTTGATCCGGCAAACAAACCACCGC
TGGTAGCGGTGGTTTTTTTGTTTGCAAGCAGCAGATTACGCGCAGAAAAAAAGGATCTC
AAGAAGATCCTTTGATCTTTTCTACGGGGTCTGACGCTCAGTGGAACGAAAACTCACGT
TAAGGGATTTTGGTCATGAGATTATCAAAAAGGATCTTCACCTAGATCCTTTTAAATTGG
AAATGAAGTTTTAAATCAATCTAAAGTATATATGAGTAAACTTGGTCTGACAGTTACCAAT
GCTTAATCAGTGAGGCACCTATCTCAGCGATCTGTCTATTTCGTTCATCCATAGTTGCCT
GACTCCCCGTCGTGTAGATAACTACGATACGGGAGGGCTTACCATCTGGCCCCAGTGC
TGCAATGATACCGCGAGACCCACGCTCACCGGCTCCAGATTTATCAGCAATAAACCAG
CCAGCCGGAAGGGCCGAGCGCAGAAGTGGTCCTGCAACTTTATCCGCCTCCATCCAG
TCTATTAATTGTTGCCGGGAAGCTAGAGTAAGTAGTTCGCCAGTTAATAGTTTGCGCAA
CGTTGTTGCCATTGCTACAGGCATCGTGGTGTCACGCTCGTCGTTTGGTATGGCTTCAT
TCAGCTCCGGTTCCCAACGATCAAGGCGAGTTACATGATCCCCCATGTTGTGCAAAAAA
GCGGTTAGCTCCTTCGGTCCTCCGATCGTTGTCAGAAGTAAGTTGGCCGCAGTGTTAT
CACTCATGGTTATGGCAGCACTGCATAATTCTCTTACTGTCATGCCATCCGTAAGATGC
TTTTCTGTGACTGGTG

bioRxiv preprint doi: https://doi.org/10.1101/2021.04.09.439171; this version posted April 10, 2021. The copyright holder for this preprint (which was not certified by peer review) is the author/funder, who has granted bioRxiv a license to display the preprint in perpetuity. It is made available under aCC-BY 4.0 International license.

Protein purifications

See Supplemental Table S3. All replication proteins were purified as in (Yeeles et al., 2015, 2017) and Polε^{exo-} was purified as in (Goswami et al., 2018). Rad53 was expressed and purified as in (Deegan et al., 2016; Gilbert et al., 2001) with an additional gel filtration step at the end in the following buffer: 25 mM HEPES-KOH, 0.02% NP-40-S, 10% glycerol, and 300 mM NaCl.

Figure 1

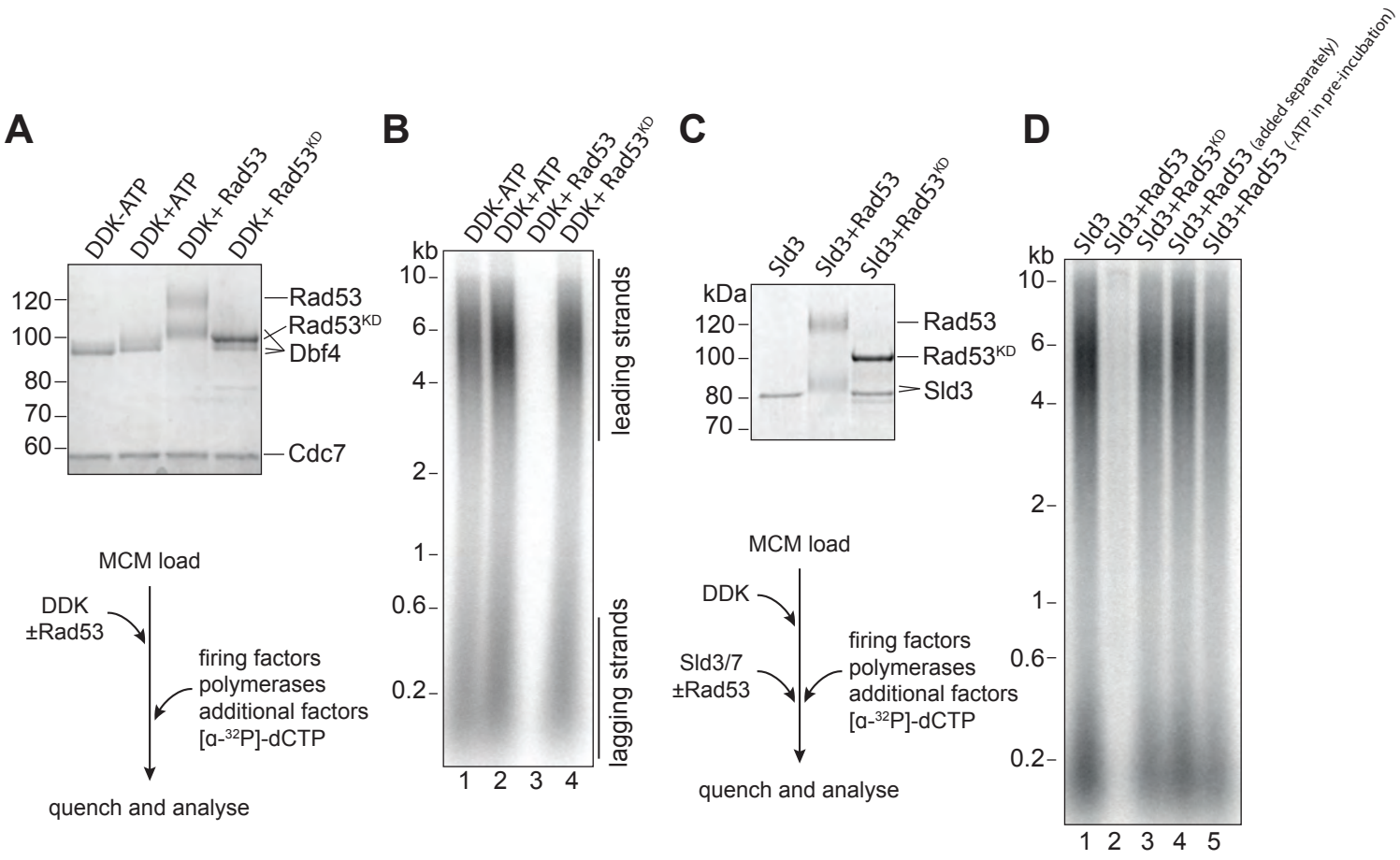
A
DDK-ATP
DDK+ATP
DDK+ Rad53
DDK+ Rad53KD
120
100
80
70
60
Rad53
Rad53KD
Dbf4
Cdc7
MCM load
DDK
±Rad53
firing factors
polymerases
additional factors
[α-32P]-dCTP
quench and analyse
B
DDK-ATP
DDK+ATP
DDK+ Rad53
DDK+ Rad53KD
kb
10
6
4
2
1
0.6
0.2
leading strands
lagging strands
1 2 3 4
C
Sld3
Sld3+Rad53
Sld3+Rad53KD
kDa
120
100
80
70
Rad53
Rad53KD
Sld3
MCM load
DDK
Sld3/7
±Rad53
firing factors
polymerases
additional factors
[α-32P]-dCTP
quench and analyse
D
Sld3
Sld3+Rad53
Sld3+Rad53KD
Sld3+Rad53 (added separately)
Sld3+Rad53 (-ATP in pre-incubation)
kb
10
6
4
2
1
0.6
0.2
1 2 3 4 5

Figure 2

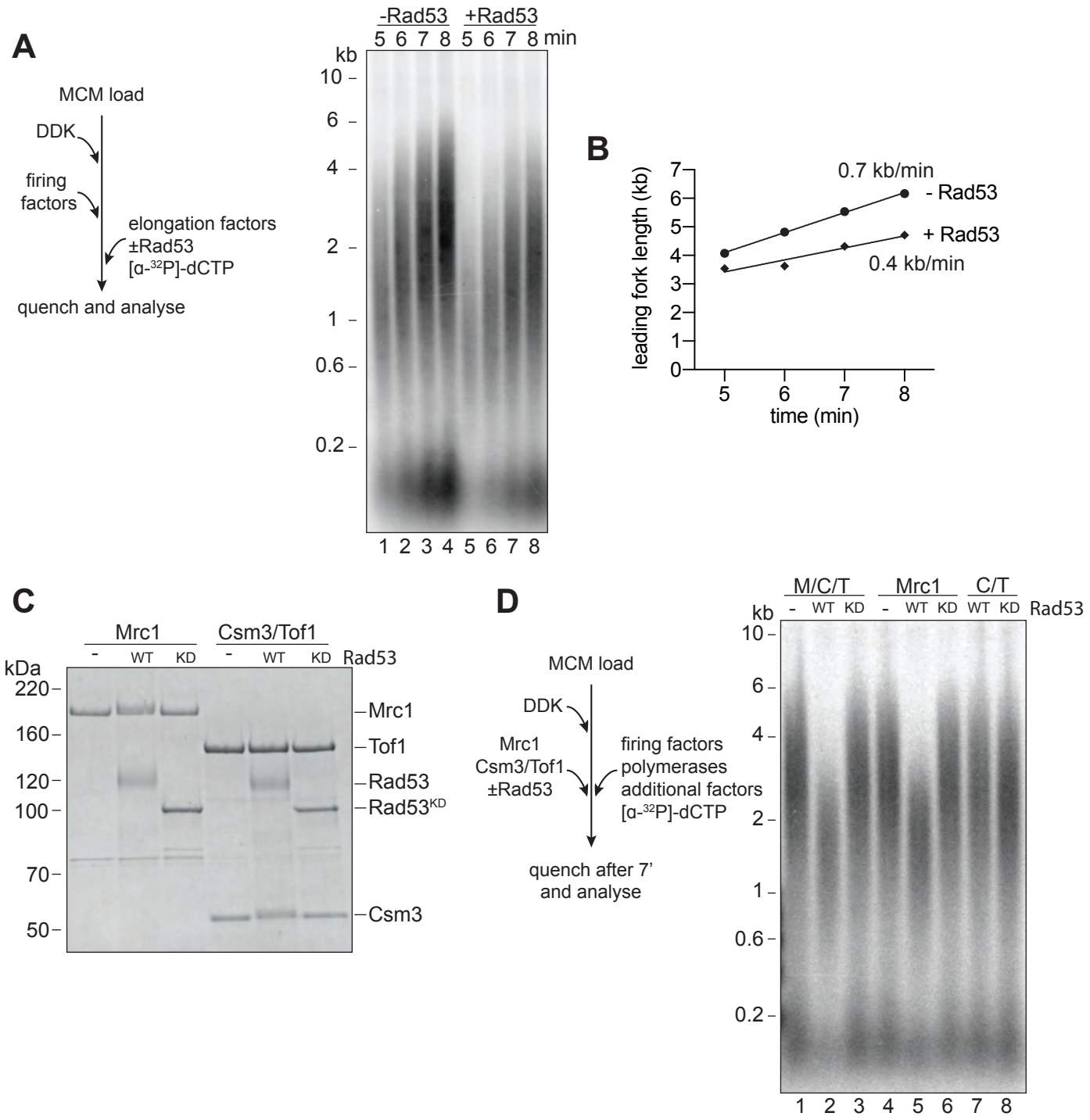
A
MCM load
DDK
firing factors
elongation factors
±Rad53
[α-32P]-dCTP
quench and analyse
-Rad53 +Rad53
5 6 7 8 5 6 7 8 min
kb
10
6
4
2
1
0.6
0.2
1 2 3 4 5 6 7 8
B
leading fork length (kb)
time (min)
0.7 kb/min
- Rad53
+ Rad53
0.4 kb/min
C
Mrc1
Csm3/Tof1
- WT KD - WT KD Rad53
kDa
220
160
120
100
70
50
Mrc1
Tof1
Rad53
Rad53KD
Csm3
D
MCM load
DDK
Mrc1
Csm3/Tof1
±Rad53
firing factors
polymerases
additional factors
[α-32P]-dCTP
quench after 7'
and analyse
M/C/T
Mrc1
C/T
kb
- WT KD - WT KD WT KD Rad53
10
6
4
2
1
0.6
0.2
1 2 3 4 5 6 7 8

Figure 3

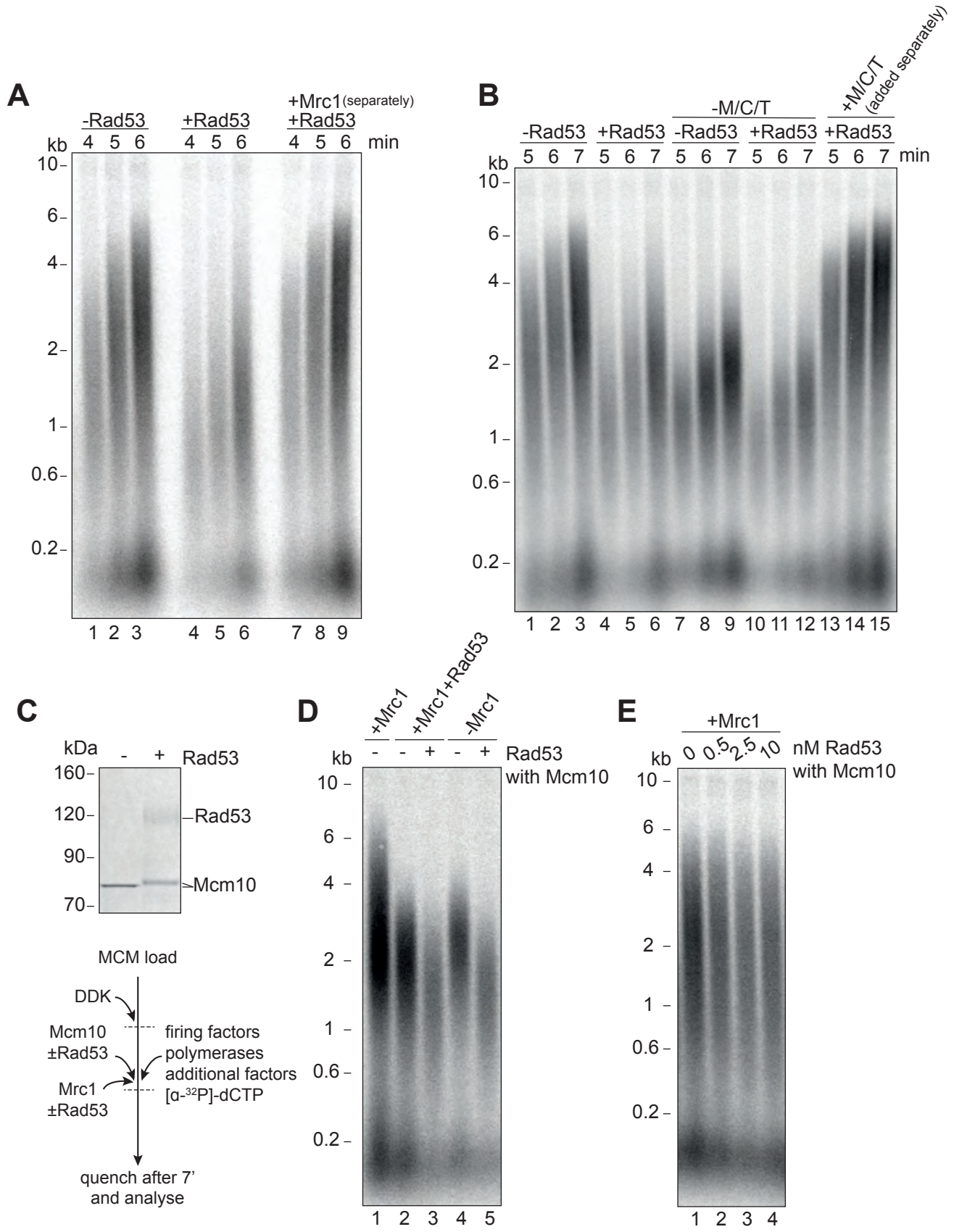
A
-Rad53
+Rad53
+Mrc1 (separately)
+Rad53
kb
4 5 6 4 5 6 4 5 6 min
10
6
4
2
1
0.6
0.2
1 2 3 4 5 6 7 8 9
B
-M/C/T
+M/C/T (added separately)
-Rad53 +Rad53 -Rad53 +Rad53 +Rad53
5 6 7 5 6 7 5 6 7 5 6 7 5 6 7 min
kb
10
6
4
2
1
0.6
0.2
1 2 3 4 5 6 7 8 9 10 11 12 13 14 15
C
kDa
- + Rad53
160
120
90
70
Rad53
Mcm10
MCM load
DDK
Mcm10 ±Rad53
Mrc1 ±Rad53
firing factors
polymerases
additional factors
[α-32P]-dCTP
quench after 7' and analyse
D
+Mrc1
+Mrc1+Rad53
-Mrc1
kb
- - + - + Rad53 with Mcm10
10
6
4
2
1
0.6
0.2
1 2 3 4 5
E
+Mrc1
kb
0 0.5 2.5 10 nM Rad53 with Mcm10
10
6
4
2
1
0.6
0.2
1 2 3 4

Figure 4

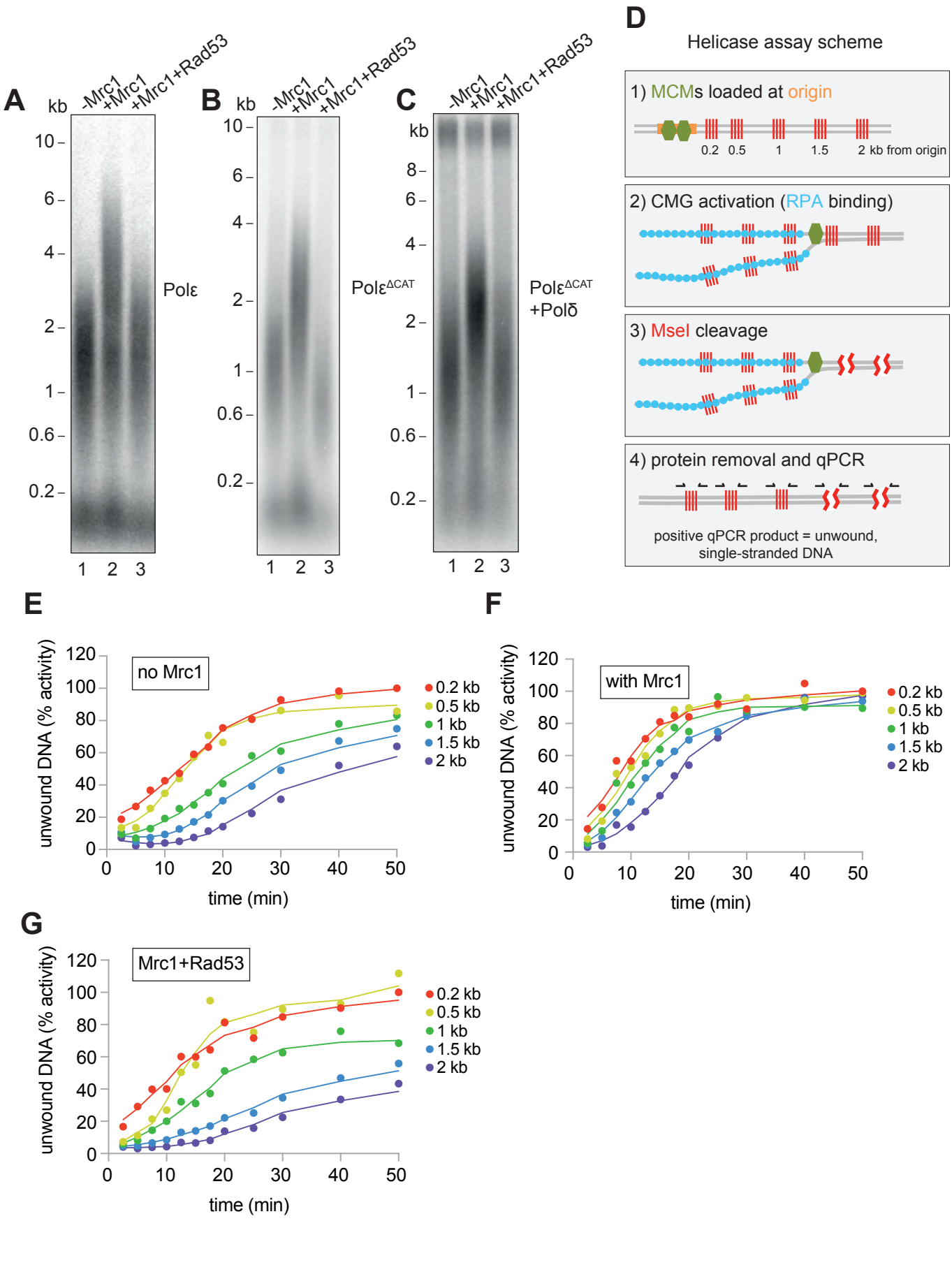
A
kb
-Mrc1
+Mrc1
+Mrc1+Rad53
10
6
4
2
1
0.6
0.2
Polε
1 2 3
B
kb
-Mrc1
+Mrc1
+Mrc1+Rad53
10
6
4
2
1
0.6
0.2
Polε^ΔCAT
1 2 3
C
kb
-Mrc1
+Mrc1
+Mrc1+Rad53
8
6
4
2
1
0.6
0.2
Polε^ΔCAT
+Polδ
1 2 3
D
Helicase assay scheme
1) MCMs loaded at origin
0.2 0.5 1 1.5 2 kb from origin
2) CMG activation (RPA binding)
3) MseI cleavage
4) protein removal and qPCR
positive qPCR product = unwound, single-stranded DNA
E
no Mrc1
unwound DNA (% activity)
time (min)
0.2 kb
0.5 kb
1 kb
1.5 kb
2 kb
F
with Mrc1
unwound DNA (% activity)
time (min)
0.2 kb
0.5 kb
1 kb
1.5 kb
2 kb
G
Mrc1+Rad53
unwound DNA (% activity)
time (min)
0.2 kb
0.5 kb
1 kb
1.5 kb
2 kb

Figure 5

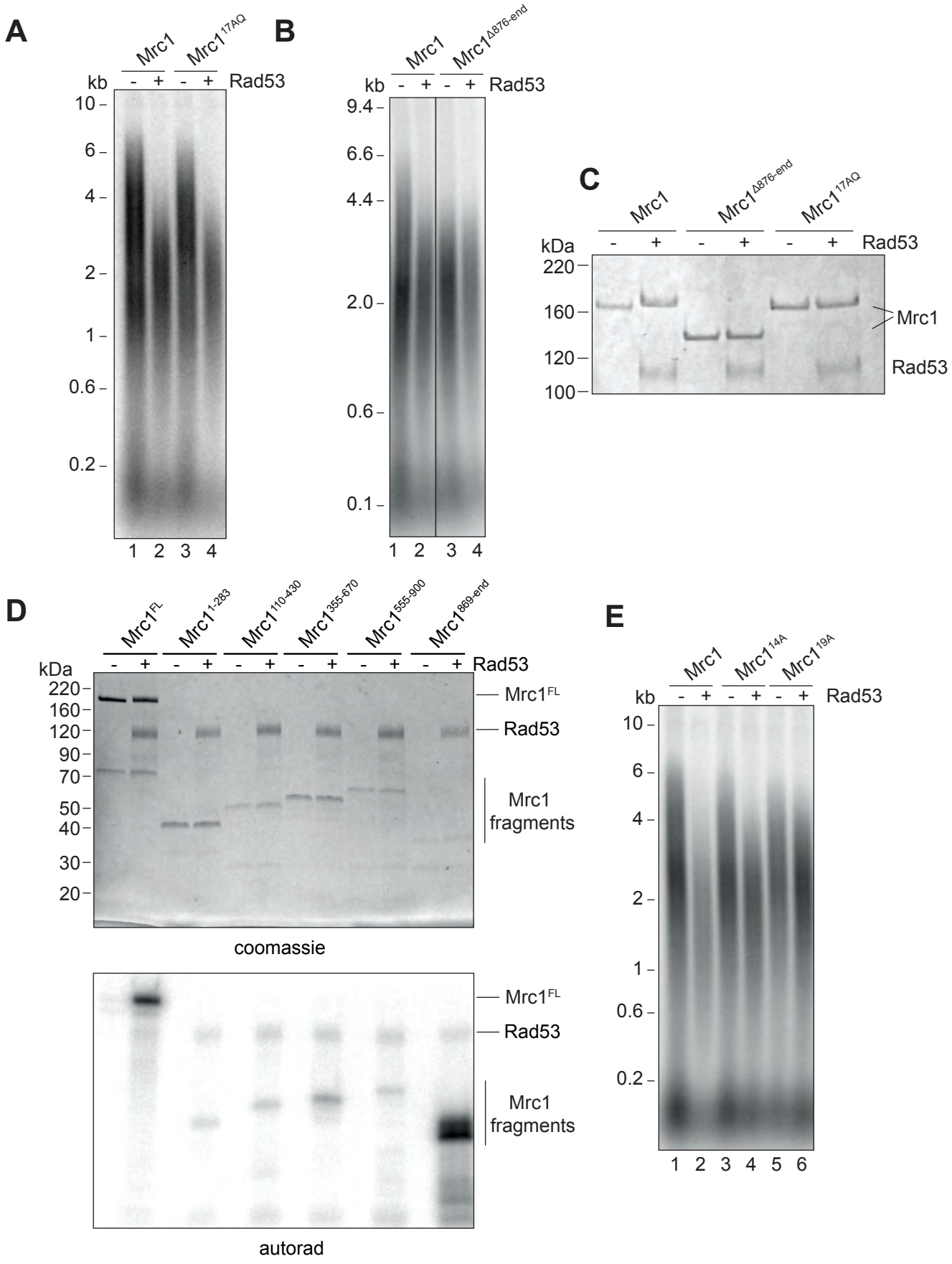
A
Mrc1
Mrc1^17AQ
kb
- + - +
Rad53
10
6
4
2
1
0.6
0.2
1 2 3 4
B
Mrc1
Mrc1^Δ876-end
kb
- + - +
Rad53
9.4
6.6
4.4
2.0
0.6
0.1
1 2 3 4
C
Mrc1
Mrc1^Δ876-end
Mrc1^17AQ
kDa
- + - + - +
Rad53
220
160
120
100
Mrc1
Rad53
D
Mrc1^FL
Mrc1^1-283
Mrc1^110-430
Mrc1^355-670
Mrc1^555-900
Mrc1^869-end
kDa
- + - + - + - + - + - +
Rad53
220
160
120
90
70
50
40
30
20
Mrc1^FL
Rad53
Mrc1 fragments
coomassie
Mrc1^FL
Rad53
Mrc1 fragments
autorad
E
Mrc1
Mrc1^14A
Mrc1^19A
kb
- + - + - +
Rad53
10
6
4
2
1
0.6
0.2
1 2 3 4 5 6

Figure 6

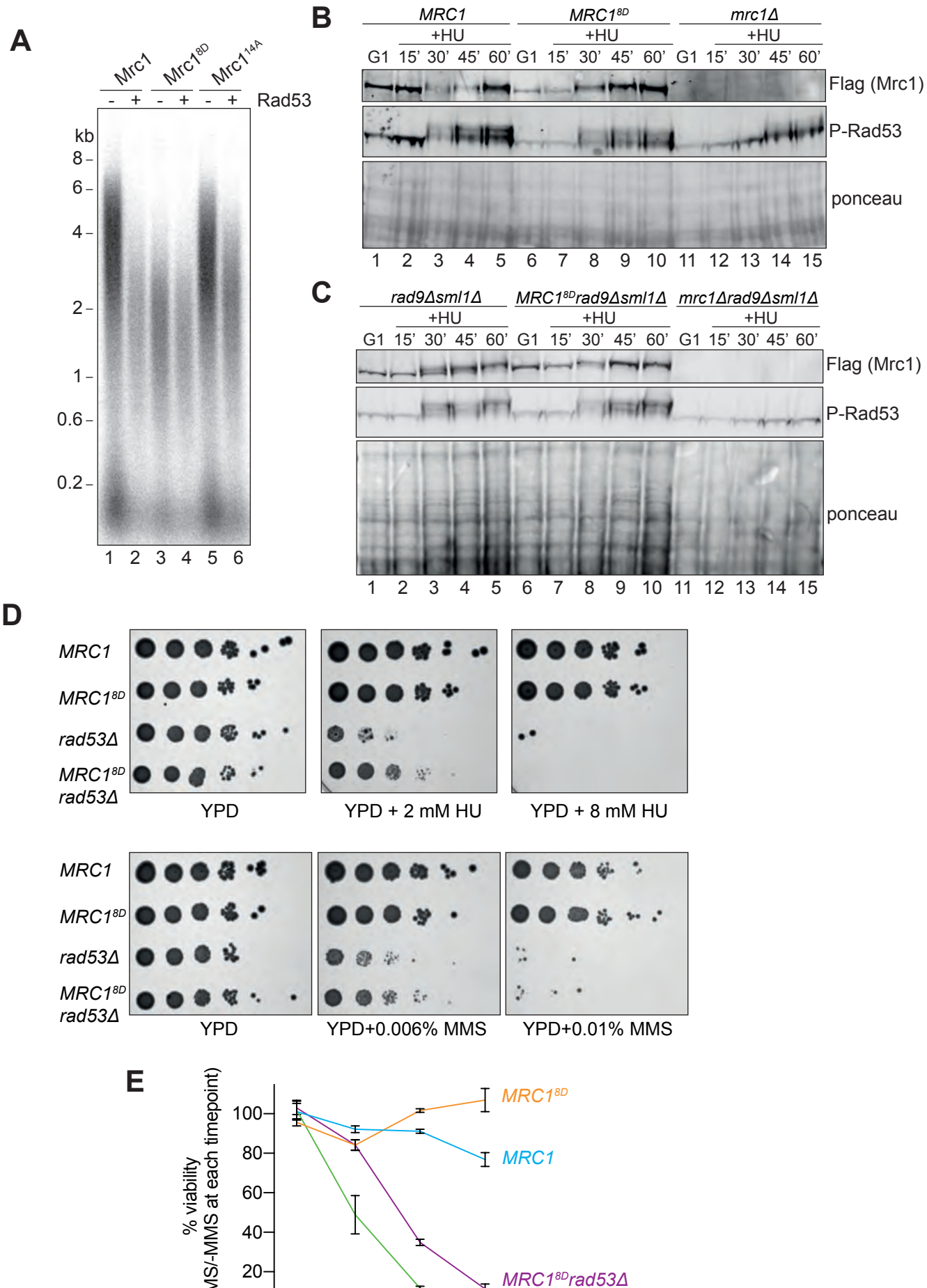
A
Mrc1
Mrc1^8D
Mrc1^14A
- + - + - +
Rad53
kb
8
6
4
2
1
0.6
0.2
1 2 3 4 5 6
B
MRC1
MRC1^8D
mrc1Δ
+HU
G1 15' 30' 45' 60' G1 15' 30' 45' 60' G1 15' 30' 45' 60'
Flag (Mrc1)
P-Rad53
ponceau
1 2 3 4 5 6 7 8 9 10 11 12 13 14 15
C
rad9Δsml1Δ
MRC1^8Drad9Δsml1Δ
mrc1Δrad9Δsml1Δ
+HU
G1 15' 30' 45' 60' G1 15' 30' 45' 60' G1 15' 30' 45' 60'
Flag (Mrc1)
P-Rad53
ponceau
1 2 3 4 5 6 7 8 9 10 11 12 13 14 15
D
MRC1
MRC1^8D
rad53Δ
MRC1^8D rad53Δ
YPD
YPD + 2 mM HU
YPD + 8 mM HU
MRC1
MRC1^8D
rad53Δ
MRC1^8D rad53Δ
YPD
YPD+0.006% MMS
YPD+0.01% MMS
E
% viability (+MMS/-MMS at each timepoint)
100
80
60
40
20
0
0 10 20 30 40 50 60 70
time (min)
MRC1^8D
MRC1
MRC1^8Drad53Δ
rad53Δ

Supplemental Figure S1

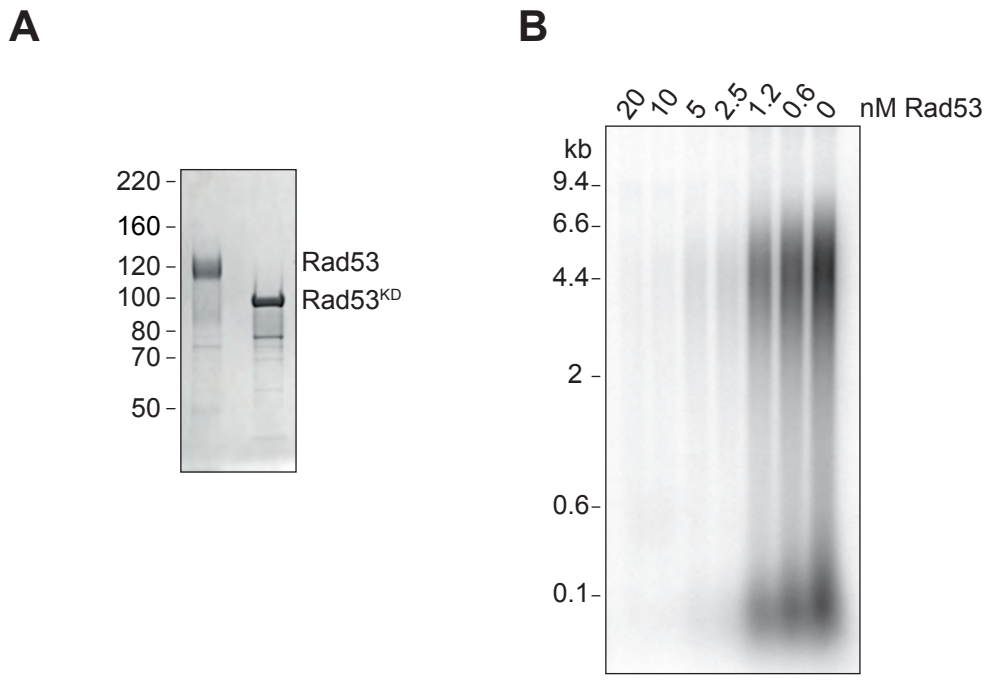

Supplemental Figure S2

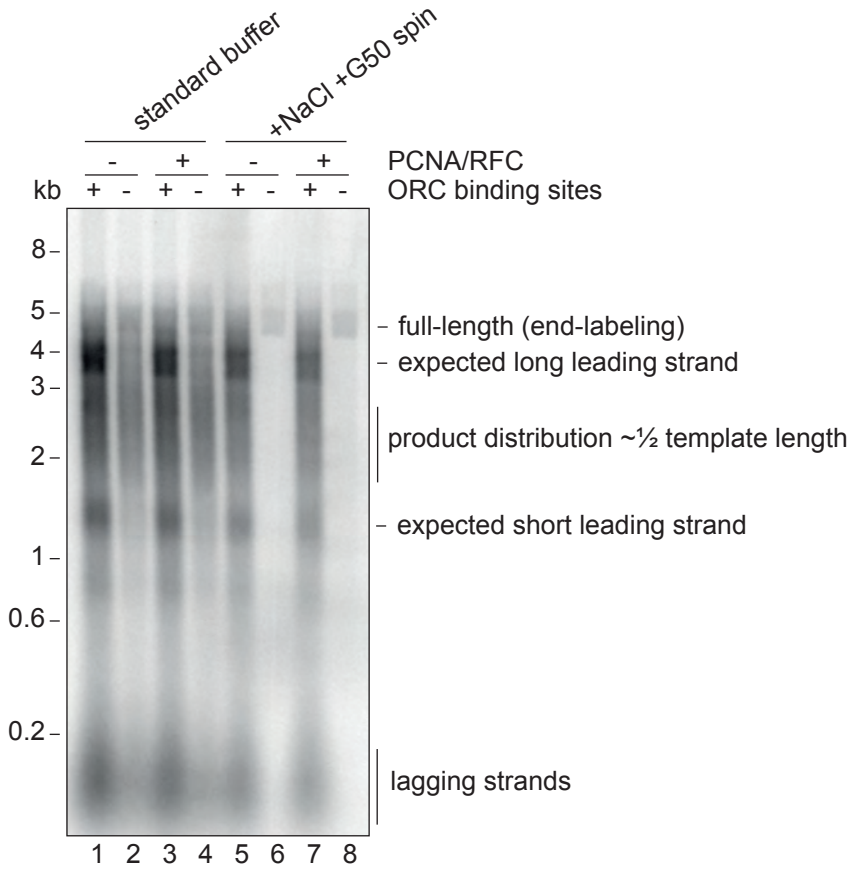

Supplemental Figure S3

A

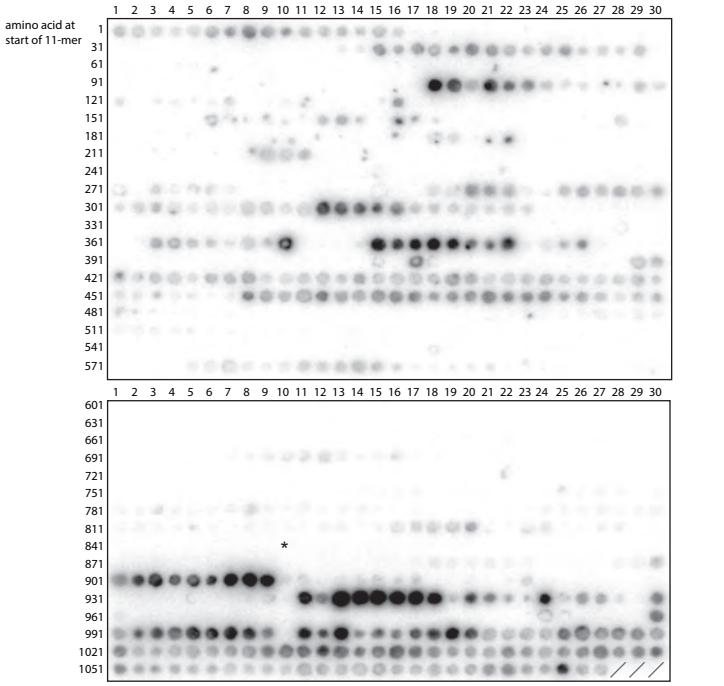

*denotes the first 20-mer that contains an amino acid from fragment 5

C

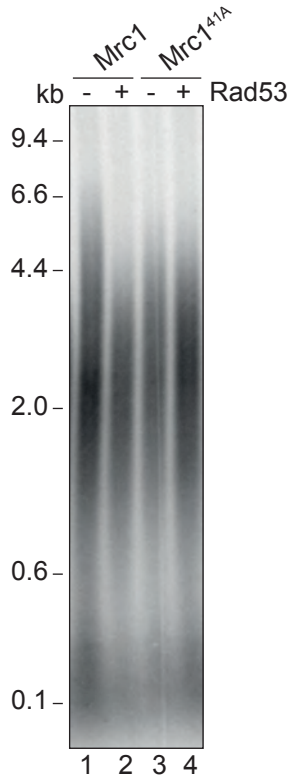

B

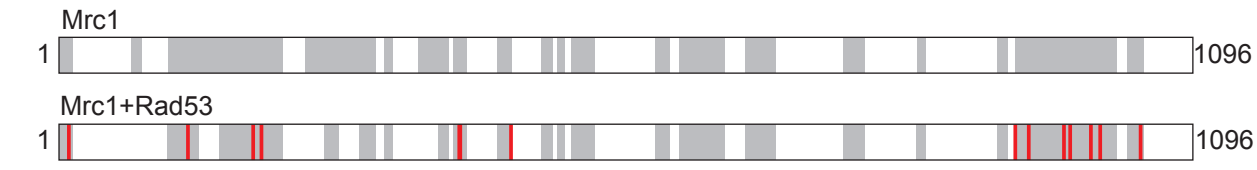

gray = peptides detected in MS
red = serines and threonines specifically phosphorylated in +Rad53 sample

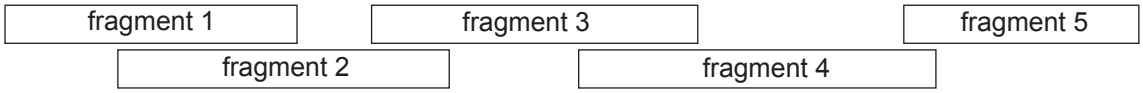

Mrc1 fragments from Figure 5D

Supplemental Figure S4